

**INVESTIGATING THE BEHAVIOUR OF TWO-PHASE VERTICAL UPWARD AND  
DOWNWARD FLOWS IN LARGE DIAMETER PIPE**

A Thesis Presented to the Department of Petroleum Engineering

African University of Science and Technology, Abuja

In partial fulfilment of the requirements for the award

**MASTER OF SCIENCE**

By

**OLARINOYE, FAWZIYAH OYEFUNKE**

Supervised by



**DR ABDULKADIR MUKHTAR**

African University of Science and Technology

[www.aust.edu.ng](http://www.aust.edu.ng)

P.M.B 681, Garki, Abuja F.C.T

Nigeria

**June, 2019**

INVESTIGATING THE BEHAVIOUR OF TWO-PHASE VERTICAL UPWARD AND  
DOWNWARD FLOW IN LARGE DIAMETER PIPE

By

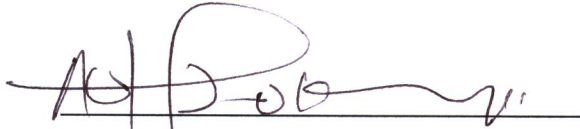
OLARINOYE, FAWZIYAH OYEFUNKE

A THESIS APPROVED BY THE PETROLEUM ENGINEERING DEPARTMENT

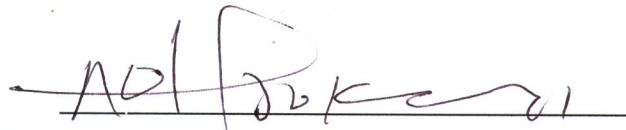
RECOMMENDED:

MA(04/07/2019)

\_\_\_\_\_  
Supervisor: Dr Abdulkadir Mukhtar

  
\_\_\_\_\_

Committee: Dr Alpheus Igbokoyi

  
\_\_\_\_\_

Head: Department of Petroleum Engineering, Dr Alpheus Igbokoyi

APPROVED:

\_\_\_\_\_  
Chief Academic Officer

\_\_\_\_\_  
Date

## **ACKNOWLEDGEMENT**

First and foremost, I give thanks to Almighty Allah for his boundless mercies, blessings and favour, without whom nothing exists or flourishes. He has been constant source of strength throughout my Master of Science program.

Secondly, I extend my profound gratitude to the World Bank and Pan African Material institute (PAMI) who provided the scholarship for my Master program. The skills I have learnt at African University of Science and Technology, Abuja through erudite professors of petroleum engineering and distinguished faculties will now be transferred for the betterment of Africa.

I sincerely thank my supervisor Dr Abdulkadir Mukhtar for his mentoring, support, and patience throughout the duration of this study. His guidance has been profoundly valuable.

I would also like to thank Dr Abdulsalami Kovo of federal University of Technology, Minna for his Support, advice and words of encouragement.

I also acknowledge the support of my family and friends: my Fiancé for his constant support and care during my study, without which it would have been impossible to carry on; Indeed I am lucky.

My sincere appreciation goes to Mohammed Isah and Adeyemi Emmanuel Adeyeye for the role they played for the successful completion of my program for strongly encouraging me.

My wonderful roommate (Asikolaye Nafisat), Ameh Peter, Kolade Emmanuel, Hanson and Helena I love you all.

Lastly I thank my course mates for the good times we had, the discussions and insights. I will forever have very fond recollections of my time with you all at AUST.

## **DEDICATION**

This work is dedicated to Almighty Allah the most gracious and the most merciful for making this M.Sc. program a success, my family: Alhaji Abdulrasaq Olarinoye, Alhaja Hawanat Olarinoye, My siblings and my ever caring and supportive Fiancé, Rasheed Nurudeen for their love, encouragement and support throughout the Program.

## TABLE OF CONTENTS

ACKNOWLEDGEMENT .....	ii
DEDICATION .....	iii
TABLE OF CONTENTS.....	iv
LIST OF FIGURES.....	vi
LIST OF TABLES.....	viii
LIST OF ABBREVIATIONS .....	ix
ABSTRACT.....	x
CHAPTER ONE .....	1
1.1 Introduction: .....	1
1.2 Problem Statement:.....	2
1.3 Aims and Objectives.....	3
1.3.1 Aims: .....	3
1.3.2 Objectives: .....	3
1.4 Structure of Thesis .....	4
CHAPTER TWO .....	5
LITERATURE REVIEW .....	5
2.1 Flow Regime.....	5
2.2 Types of Flow Regime in Horizontal and Vertical Pipe .....	5
2.3 Flow Pattern Maps.....	11
2.4 Void Fraction and Liquid Hold Up .....	13
2.4.1 Liquid hold up: .....	13
2.4.2 Void fraction:.....	14
2.4.3 Void fraction correlation:.....	15
2.4.4 Void fraction correlation based on momentum balance:.....	16
2.4.5 Drift Flux Model constitutive equations: .....	17
2.5 Power Spectrum Density (PSD):.....	18
CHAPTER THREE .....	20
METHODOLOGY .....	20
3.1 Data Acquisition:.....	20
3.2 Data Processing:.....	20
3.3 Data Analysis:.....	21
3.4 Identification of Downward Flow Regime: .....	21
3.5 1-D Drift Flux Model:.....	21

3.6 Analysis of Performance of Void Fraction Correlations and Validation Of $C_o$ and $U_{GM}$	
Constitutive Equations:.....	22
CHAPTER FOUR .....	24
Results and Discussion: .....	24
4.1 Time Series of Void Fraction: .....	24
4.2 Probability Density Function (PDF): .....	26
4.3 Flow pattern Map: .....	27
4.4 Variation of Averaged Void Fraction on Liquid and Gas Superficial Velocity: .....	28
4.5 Effect of Frequency on Gas and Liquid Superficial Velocity:.....	33
4.6: Effect of Gas Actual Velocity on Mixture Velocity (Drift-Flux Model): .....	36
4.7: Analysis of the Performance of Void Fraction Correlations: .....	38
4.8 Root Mean Error: .....	43
4.9: Validation of the Constitutive Equations for $C_o$ and $U_{GM}$ :.....	48
CHAPTER 5 .....	50
Conclusion:.....	50
REFERENCES .....	52

## LIST OF FIGURES

<b>Fig 2.1:</b> flow pattern map in Horizontal flow (Alireza, 2014).....	6
<b>Fig 2.2:</b> flow regime in vertical flow (Alireza, 2014) .....	8
<b>Fig 2.3:</b> (Oshinowo, 1972) vertical downward flow pattern map (adapted from (Almabrok, 2013)) ..	11
<b>Fig 2.4:</b> (Yamazaki & Yamaguchi, 1979)flow pattern map for vertical flow .....	12
<b>Fig 2.5:</b> (Paras, 1982) vertical flow pattern map (adapted from (Almabrok, 2013)) .....	12
<b>Fig 2.6:</b> (Yijun & Rezkallah, 1993) flow pattern map (adapted from (Almabrok, 2013)) .....	13
.....	23
<b>Fig 3.1:</b> Flow chart of the Methods.....	23
<b>Fig 4.1(a):</b> Time series for air-water flow for vertical upward at $U_{SL}$ of 0.08m/s and $U_{SG}$ of 9.92m/s...	24
<b>Fig 4.1(b):</b> Time series for air-water flow in vertical downward at $U_{SL}$ of 0.08m/s and $U_{SG}$ of 9.92m/s	25
<b>Fig 4.2a:</b> PDF for air-water flow in vertical upward at $U_{SL}$ of 0.08m/s and $U_{SG}$ of 9.92m/s.....	26
<b>Fig 4.2b:</b> PDF for air-water flow in vertical downward at $U_{SL}$ of 0.08m/s and $U_{SG}$ of 9.92m/s.....	26
<b>Fig 4.3a:</b> Flow pattern map for vertical upward flow .....	28
<b>Fig 4.3b:</b> Flow pattern map for vertical downward flow .....	28
<b>Fig 4.4a:</b> plot of average void fraction versus gas superficial velocity at $U_{SL}$ of 0.02m/s .....	29
<b>Fig 4.4b:</b> plot of average void fraction versus gas superficial velocity at $U_{SL}$ of 0.04m/s .....	29
<b>Fig 4.4c:</b> plot of average void fraction versus gas superficial velocity at $U_{SL}$ of 0.08m/s.....	30
<b>Fig 4.4d:</b> plot of average void fraction versus gas superficial velocity at $U_{SL}$ of 0.1m/s .....	30
<b>Fig 4.4e:</b> plot of average void fraction versus gas superficial velocity at $U_{SL}$ of 0.2m/s .....	30
<b>Fig 4.5a:</b> plot of dominant frequency versus gas superficial velocity at $U_{SL}$ =0.02m/s .....	33
<b>Fig 4.5b:</b> plot of dominant frequency versus gas superficial velocity at $U_{SL}$ =0.04m/s .....	34
<b>Fig 4.5c:</b> plot of dominant frequency versus gas superficial velocity at $U_{SL}$ =0.08m/s.....	34
<b>Fig 4.5d:</b> plot of dominant frequency versus gas superficial velocity at $U_{SL}$ =0.1m/s .....	35
<b>Fig 4.5e:</b> plot of dominant frequency versus gas superficial velocity at $U_{SL}$ =0.2m/s .....	35
<b>Fig 4.6(a):</b> Drift-flux model for vertical downward flow .....	36
<b>Fig 4.6(b):</b> Drift-flux model for vertical upward flow.....	36
<b>Fig 4.7(a):</b> performance of 11 correlations for vertical upward air-water flow at $U_{SL}$ of 0.02m/s .....	39
<b>Fig 4.7(b):</b> performance of 11 correlations for vertical downward air-water flow at $U_{SL}$ of 0.02m/s..	40
<b>Fig 4.7(c):</b> performance of 11 correlations for vertical upward air-water flow at $U_{SL}$ of 0.04m/s .....	40
<b>Fig 4.7(d):</b> performance of 11 correlations for vertical downward air-water flow at $U_{SL}$ of 0.04m/s..	40
<b>Fig 4.7(e):</b> performance of 11 correlations for vertical upward air-water flow at $U_{SL}$ of 0.08m/s .....	41
<b>Fig 4.7(f):</b> performance of 11 correlations for vertical downward air-water flow at $U_{SL}$ of 0.08m/s...	41
<b>Fig 4.7(g):</b> performance of 11 correlations for vertical upward air-water flow at $U_{SL}$ of 0.1m/s .....	41

<b>Fig 4.7(h):</b> performance of 11 correlations for vertical downward air-water flow at $U_{SL}$ of 0.1m/s....	42
<b>Fig 4.7(i):</b> performance of 11 correlations for vertical upward air-water flow at $U_{SL}$ of 0.2m/s.....	42
<b>Fig 4.7(j):</b> performance of 11 correlations for vertical downward air-water flow at $U_{SL}$ of 0.2m/s.....	43
Fig 4.8 (a): RMSE value for 11 correlations for Up and down flow for $U_{SL}=0.02\text{m/s}$ .....	43
Fig 4.8(b): RMSE value for 11 correlations for Up and down flow for $U_{SL}=0.04\text{m/s}$ .....	44
Fig 4.8(c): RMSE value for 11 correlations for Up and down flow for $U_{SL}=0.08\text{m/s}$ .....	44
Fig 4.8(d): RMSE value for 11 correlations for Up and down flow for $U_{SL}=0.1\text{m/s}$ .....	44
Fig 4.8(e): RMSE value for 11 correlations for Up and down flow for $U_{SL}=0.2\text{m/s}$ .....	45

## LIST OF TABLES

Table 2.1: 10 top performing correlations for vertical downward and upward two-phase flow (Bhagwat & Ghajar, 2012a) based on concept of drift-flux.....	16
<b>Table 2.2:</b> constitution equation for drift-flux related to large diameter pipes.....	18
Table 4.1: Physical properties of air-water at test conditions .....	24
<b>Table 4.2:</b> Distribution parameters and Drift velocity for Vertical upward and downward flows .....	37
<b>Table 4.3:</b> Comparison of prediction of void fraction correlations in vertical upward air-water flow	45
<b>Table 4.4:</b> Comparison of prediction of void fraction correlations in vertical downward air-water flow .....	46

## LIST OF ABBREVIATIONS

<b>Symbol</b>	<b>Description</b>	<b>Unit</b>
A	Area	m <sup>2</sup>
D	Diameter	M
G	Acceleration due to gravity	m/s <sup>2</sup>
U <sub>SG</sub>	Superficial gas velocity	m/s
U <sub>SL</sub>	Superficial liquid velocity	m/s
U <sub>L</sub>	Actual liquid velocity	m/s
U <sub>G</sub>	Actual gas velocity	m/s
U <sub>M</sub>	Mixture velocity	m/s
U <sub>GM</sub>	Drift velocity	m/s
C <sub>o</sub>	Distribution coefficient	Dimensionless
E	Void fraction	%
H <sub>L</sub>	Liquid hold up	%
L	Length	M
P	Pressure	Pa
Δρ	Density difference	Kg/m <sup>3</sup>
ρ <sub>L</sub>	Liquid density	Kg/m <sup>3</sup>
ρ <sub>G</sub>	Gas density	Kg/m <sup>3</sup>
F	Frequency	Hertz (Hz)
M	<b>Viscosity</b>	<b>Pa-s</b>
Σ	Surface tension	N/m
C <sub>w</sub>	<b>Wall friction factor</b>	<b>Dimensionless=0.005</b>
Fr <sub>L</sub>	Liquid Froude number	Dimensionless
PDF	<b>Probability density function</b>	
PSD	Power spectrum density	
T	Time	Second (s)

## ABSTRACT

The understanding of the behaviour of vertical upward and downward two-phase flow in large diameter pipes is very important in chemical, petroleum and nuclear sector where safety is of utmost concern. This work helps to add to the little research done on vertical downward flow in large diameter pipes as compared to numerous works done in vertical upward flow. This work analysed the experimental results obtained from using a conductance ring probe of the void fraction measurements done on air-water flow in 127mm diameter pipe for vertical upward and downward. A gas superficial velocity ( $U_{SG}$ ) and liquid superficial velocity ( $U_{SL}$ ) ranges from (3.45-16.05) m/s and (0.02-0.2)m/s respectively. Annular flow regime was identified in vertical upward and downward flow with the use of the probability density function (PDF), time series of average void fraction and Sholam's flow pattern map and the result was compared with previous studies. The analysis of the 15000 data points for the 17 runs for the upward and downward flow showed tendency in the effect of void fraction and dominant frequency with varying flow rates. The differences in the behaviour of the vertical upward flow and vertical upward flow observed were as a result of the gravity, buoyancy and interaction of the liquid inertia. Using the drift flux model, the linear relationship between the gas actual velocity and mixture velocity was established for both pipe orientations for  $U_{SL}$  of (0.02-0.2)m/s to give the distribution parameter ( $C_o$ ) and drift velocity ( $U_{GM}$ ). The available drift-flux models developed for vertical upward flow can be equally used for downward flow by changing the sign of the drift velocity from positive to negative. The result of the top 10 drift-flux model correlations and the one derived from momentum equation for falling film/annular flow available for upward flow and downward flow to predict the void fraction were used and compared to the one in this work to check for the percentage error and RMS error.

**Keywords:** Upward, downward, dominant frequency, two-phase flow, drift-flux, momentum equation, inertia, buoyancy, gravity, annular flow, falling film flow, drift velocity, distribution parameter, conductance probe, void fraction and Superficial velocity.

## CHAPTER ONE

### 1.1 Introduction:

The long transportation of a liquid or gas and any chemical stable substances typically to a market area for consumption are sent through pipeline when it needs to move over hills or where canals or channels are poor choices due to considerations of evaporation, pollution, or environmental impact. Pipes are defined as Flow sections of circular cross section. Most fluids, especially liquids, are transported in circular pipes this is because pipes with a circular cross section can withstand large pressure due to differences between the inside and the outside without undergoing significant distortion. Fluids flow through pipes for the purpose of fluid distribution, heating and cooling applications. A typical piping system involves pipes of different diameters (small or large) connected to each other by various fittings or elbows to route the fluid, valves to control the flowrate, and pumps to pressurize the fluid. Small diameter pipes are usually referred to as tubes where Taylor bubbles which characterised slug flow regime can be easily observed is defined by (Shen, X. et al., 2014) as pipe whose  $D_H^*$  is less than 18 (Capovilla, Coutinho, de Sousa, & Waltrich, 2019) while (Kataoka & Ishii, 1987) defined a large diameter pipe as a pipe whose diameter is greater than the maximum cap bubble size (Wang, Li, Yang, & Ishii, 2018) where Taylor bubble cannot be sustained as:

$$D_H^* \equiv \frac{D_H}{\sqrt{\frac{\sigma}{g\Delta\rho}}} \geq 40$$

However, the bubble behaviour, void fraction and velocity profiles in large pipes can be very different in small pipes and can cause different physical mechanisms of gas and liquid transport which makes models in small diameter pipes not suitable for large diameter pipes (Wang, Li, Yang, et al., 2018).

The problem arising from mixture of two fluids through pipes is the issue of multiphase flow and understanding this phenomenon will help solve the problem. Flow instabilities may

cause the mixture to arrange itself into different geometric configurations. These geometric configurations are usually referred to as flow patterns. Because of the role played by gravity, the density difference between the two fluids, void fraction, gas and liquid flowrates, the orientation of the pipe either horizontal or vertical (upward and downward) and its diameter always makes a difference in the flow pattern. The difficulty of the structure of two-phase flow is due to complexity of the form in which the fluids exist. Basically, flow regimes that are formed in either vertical or horizontal pipes occur due to co-production of oil and gas, water vaporisation and fluid mixing in the pipeline.

In order to identify two-phase flow regime, methods such as visual observation done by using high speed camera, analysis of averaged void fractions are used (Dong, Liu, Deng, Xu, & Xu, 2001).

The principal importance of the knowledge of two-phase flow in large diameter pipes occur in area of nuclear industry, energy sector, petroleum industry, and chemical engineering for nuclear safety, heat transfer, transportation of oil and natural gas and mass transport respectively.

## **1.2 Problem Statement:**

Hitherto research concerning two phase vertical flow was dedicated to upward flow with little attention paid to vertical downward flow. In addition, there are a lot of data concerning two-phase vertical flows in small diameter pipes that have evolved over the years. Unfortunately, there is a dearth of data for vertical downward flow in large diameter pipes when compared to work done on vertical upward flow.

Although downward vertical two-phase flow is less common than upward flow, it does occur in steam injection wells and down comer pipes from offshore production platforms. Hence a general vertical two-phase flow pattern is required that can be applied to all flow situations. Reliable models for downward two-phase flow are currently unavailable and the design codes are deficient in this area.

The main drive in this work is to:

- Compare the behaviour of air-water vertical flow in both upward and downward flow using the analysed data.
- Look for models that best predicts the behaviour of air-water flow in vertical upward and downward flow with more emphasis on vertical downward flow.

### **1.3 Aims and Objectives**

#### **1.3.1 Aims:**

The aim of the study is to investigate the behaviour of vertical air-water upward and downward flows in a large diameter pipe.

#### **1.3.2 Objectives:**

To achieve this aim, the following objectives will be met:

- Process and analyse the raw experimental data obtained from conductance ring probes.
- To use a flow pattern map to determine the prevailing flow regimes in vertical upward flow and vertical downward flows at the same conditions.
- Interrogate the effect of liquid and gas superficial velocities on void fraction for vertical upward and vertical downward flows.
- Compare the values of void fraction for vertical upward against vertical downward flow at the same operating conditions.
- Determine and compare the frequency and actual velocity for vertical upward and downward flow at the same conditions.
- Compare some selected published empirical correlations against experimental data for vertical upward and vertical downward flow.

#### **1.4 Structure of Thesis**

- Chapter one will provide the introduction, the aim and objectives of this work
- Chapter two of this thesis will provide a review of some important literatures on this topic.
- Chapter three will focus on processing and analysis of raw experimental data gathered from the University of Nottingham, United Kingdom.
- Chapter four will focus on presentation of results and discussion of the analysed data from chapter three
- Chapter five is conclusion and recommendation
- References

## CHAPTER TWO

### LITERATURE REVIEW

#### 2.1 Flow Regime

Flow regime otherwise known as flow pattern can be defined as the description of the flow structure, or the distribution of one fluid phase relative to another (Alireza, 2014). The determination of flow regime gives an important clue whether or not top-of-the-line corrosion can be an issue (Singer, 2017). It can be encountered in horizontal, vertical upward or vertical downward two-phase flow.

The flow regimes encountered in either vertical upward or downward two-phase flow are often less complex than those in horizontal flow which is as a result of the symmetry in the flow caused by gravitational force acting parallel to it. It should be noted that vertical flows are not so common in raw natural gas systems because the wells used to have some deviation and many risers are inclined to some extent. These flow regimes can be bubble flow, slug flow, churn flow and annular flow (Mokhatab & Mak, 2015).

The interaction between the liquid inertia, buoyancy, gravity and surface tension in two phase flow is symmetrical about the pipe axis. Over the years less concentration is given to downward configuration but a lot of research has been done in the field of flow patterns and void fractions involving vertical upward two phase flow. The drift-flux and the two-fluid model are the two most common models used to formulate a general transient two-phase flow model.

#### 2.2 Types of Flow Regime in Horizontal and Vertical Pipe

A flow regime (or flow pattern) is essentially a description of the flow structure, or distribution of one fluid phase relative to the other (Alireza, 2014). In horizontal oil and gas pipe lines three (3) major three-phase flow regimes are commonly encountered:

- **Stratified flow:** Segregation of the gas and liquid phases, usually at low gas and liquid flow rates.
  - **Intermittent flow:** Formation of slugs or plugs at high liquid flow rates as the crests of the waves intermittently reach the top of the pipe.
  - **Annular flow:** The bulk liquid phase is partly atomized at high gas flow rate, leading to transport and deposition of droplets to the whole circumference of the pipe.
- (Singer, 2017)

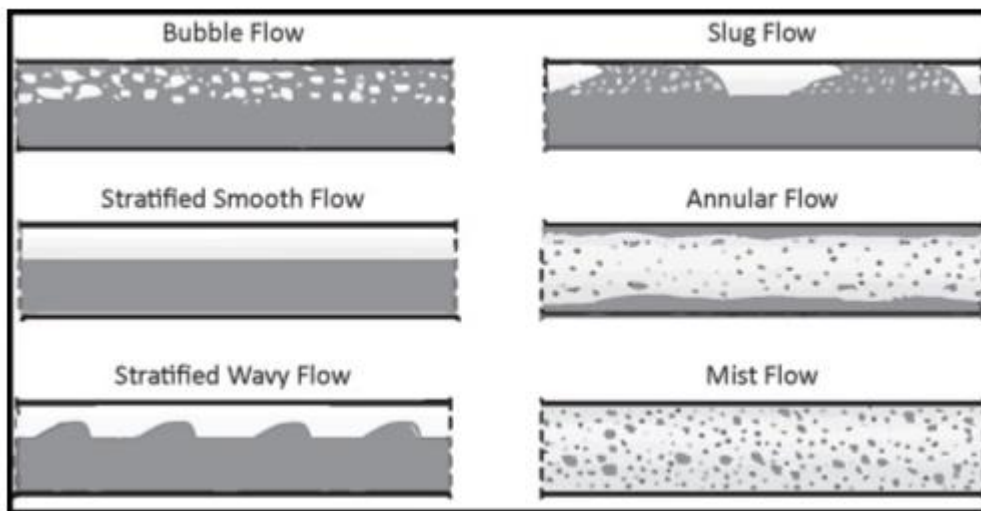


**Fig 2.1:** flow pattern map in Horizontal flow (Alireza, 2014)

(Mokhatab & Mak, 2015) explains vertical flow regimes as flow regimes frequently encountered in upward vertical two-phase flow. These flow regimes tend to be somewhat simpler than those in horizontal flow. This results from the symmetry in the flow induced by the gravitational force acting parallel to it. A brief description of the manner in which the fluids are distributed in the pipe for upward vertical two-phase flow is as follows:

- **Bubble flow:** at very low liquid and gas velocities, the liquid phase is continuous and the gas phase travels as dispersed bubbles. This flow regime is called bubble flow. As the liquid flow rate increases, the bubbles may increase in size via coalescence. Based on the presence or absence of slippage between the two

phases, bubble flow is further classified into bubbly and dispersed bubble flows. In bubbly flow, relatively fewer and larger bubbles move faster than the liquid phase because of slippage. In dispersed bubble flow, numerous tiny bubbles are transported by the liquid phase, causing no relative motion between the two phases.

- **Slug flow:** As the gas velocity increases, the gas bubbles start coalescing, eventually forming large enough bubbles (Taylor bubbles) which occupy almost the entire cross-sectional area. This flow regime is called slug flow. Taylor bubbles move uniformly upward and are separated by slugs of continuous liquid that bridge the pipe and contain small gas bubbles. Typically, the liquid in the film around the Taylor bubbles may move downward at low velocities although the net flow of liquid can be upward. The gas bubble velocity is greater than that of the liquid.
- **Churn (transition) flow:** it is a change from a continuous liquid phase to a continuous gas phase occurs; the continuity of the liquid in the slug between successive Taylor bubbles is repeatedly destroyed by a high local gas concentration in the slug. This oscillatory flow of the liquid is typical of churn (froth) flow. It may not occur in small diameter pipes. The gas bubbles may join and liquid may be entrained in the bubbles. In this flow regime, the falling film of the liquid surrounding the gas plugs cannot be observed.
- **Annular flow:** As the gas velocity increases even further, the transition occurs and the gas phase becomes a continuous phase in the pipe core. The liquid phase moves upward partly as a thin film (adhering to the pipe wall) and partly in the form of dispersed droplets in the gas core. This flow regime is called an annular flow or an annular-mist flow.

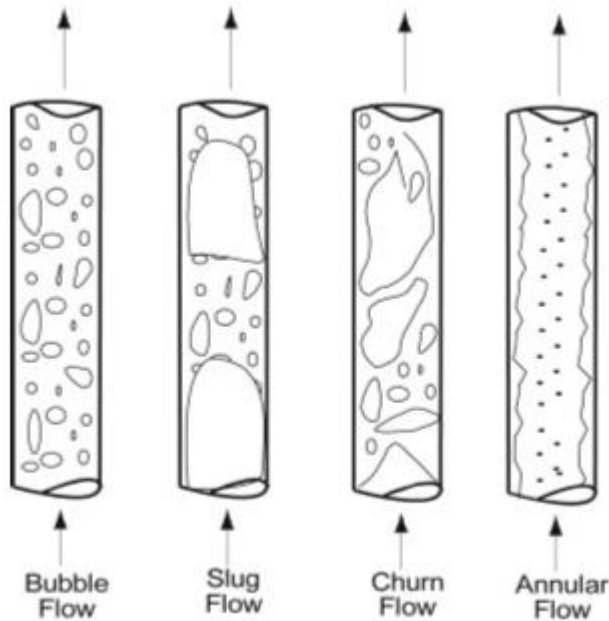


**Fig 2.2:** flow regime in vertical flow (Alireza, 2014)

The aim of this chapter is to highlight the flow patterns and general agreement or discrepancies in the investigation done so far by different researchers on vertical downward two-phase flow in large diameter pipes using air-water fluid combination, followed by a brief discussion on flow pattern maps. The latter part of this chapter will report on the investigation in the field of void fraction correlations.

(Bhagwat & Ghajar, 2012b) carried out experiments on vertical upward and vertical downward two-phase flow by measuring the flow patterns and the void fractions. They also observed a definite difference in the appearance of the upward and vertical two phase flow as a result of the interaction of the liquid inertia and the buoyancy force. They observed that there is a tendency in the variation of void fraction with varying flow rate from the analysis of the 1208 and 909 experimental data points for the upward and downward flow. They compared the upward and downward two phase flow which was done in terms of the flow patterns and void fraction values. The study of flow patterns for the upward and downward configuration has shown significant differences in the emergence of bubbly and slug flow regimes. In vertical downward orientation, there is no appearance of churn flow but only appearance of falling film flow. For the interaction of the buoyancy, gravity and liquid inertia

forces also shown difference in terms of upward and vertical two phase flow which is as a result of difference in void fraction between the two orientations. From the concept of drift flux model using different correlations, they were able to predict the void fraction in downward orientation by flipping the sign of the drift velocity from positive to negative and vice versa.

(Wang, Li, Yang, et al., 2018) investigated flow regimes and their transitions in downward two phase flow experiment using 203.2mm diameter pipe by measuring the void fraction using the arc-type and ring type impedance meters. They observed that three flow regimes such as cap-bubbly, churn-turbulent and annular flow were detected in downward flow while three flow regimes such as stratified, plug and pseudo-slug flow were observed in horizontal section. From their work, they concluded that cap bubbles could be observed even at very low void fraction and that large diameter results in the absence of slug flow but unstable slugs have been observed as the transition from cap-bubbly flow to annular flow. Probability density function (PDF) and cumulative probability density function (CPDF) of area averaged void fraction signals were used as pointers for self-organised neural network (SONN) for identification for horizontal and vertical flow regimes respectively. They compared downward flow regimes map for 203.2mm diameter pipes with that of different diameter pipe sizes. The result have shown that flow regime maps flow regime maps agree well with that of pipe size 101.6mm but do not agree well with pipe sizes as small as 25.4mm and 50.8 mm. they concluded that regardless of the superficial gas velocity, it is found that transition between churn-turbulent and annular flow occurs at particular superficial liquid velocity.

(Wang, Li, Yang, et al., 2018) performed experiment on air-water downward two phase flow in 203.2mm diameter pipe using area-averaged void fraction and pressure measurement as well as flow visualisation at several axial locations for three flow regimes which are cap-bubbly, churn-turbulent flow and annular flow. From their work, they performed experiment for superficial gas and superficial liquid velocity for different flow conditions ranging from 0.05m/s to 0.03m/s and 0.1m/s to 1.5m/s respectively for the three flow regimes. It was

concluded that due to buoyance effect on gas phase in the vertical section, the void fraction and flow structure in the top and bottom horizontal section can be quite different. At low superficial gas velocity (0.05-0.03m/s) and moderate superficial liquid velocity (1-1.2m/s) large cap-bubbles moving upward can be observed. At a value of superficial liquid velocity less than that of a critical value, annular (falling film) flow is observed in the vertical downward part. Also, in falling film flow it is observed that the void fraction is almost independent of the superficial gas velocity. The collected data were evaluated using the drift-flux models. For a value of void fraction less than 0.3 of the cap-bubbly flow conditions agrees well with the model while a value of void fraction greater than 0.3 indicates a larger drifts velocity of the churn-turbulent flow conditions than the model developed.

(Yang, Dang, Yang, Ishii, & Shan, 2018) performed an experiment on a piping system with an inner diameter of 152.4 mm by using the artificial neural network to classify the four flow patterns (bubbly flow, cap-bubbly flow, churn-turbulent flow and annular flow) and the probability density function (PDF) is discussed. Existing criteria for a downward flow regime boundary are reviewed and compared with the experiment. They come to conclusion that not all existing criteria can be applied on large pipes but lee's criteria have predicted the boundary between the cap-bubbly flow and churn-turbulent flow. In their work they proposed several criteria that for the boundary between the bubbly flow and the cap-bubbly flow, a critical value of 0.05 of void fraction is proposed. Lee's criteria are recommended for boundary between cap-bubbly and churn-turbulent flow. For pipes whose diameter is greater than 24mm and less than 101.6mm a general empirical correlation for critical void fraction has been proposed for boundary between cap-bubbly flow and slug flow. Film thickness can be used to the boundary of the falling film flow regime. The wave amplitude is big enough to form a liquid bridge when the mean film thickness is greater than  $0.0528D$ . The criterion cannot be applied if a sparger is used to inject gas into the test section in which the inlet effect affects the boundary greatly. Because the boundaries found in different experiment cannot agree well with each other, the annular mist regime boundary is not discussed in this

paper so no criterion for the boundary is found. However, Crawford's empirical correlation was recommended.

### 2.3 Flow Pattern Maps

The graphical representation of different flow patterns with varying flow rates of two phases is termed the flow pattern map. It is the plot of flow parameters such as mass flow rates, superficial velocities, mass fluxes or dimensionless parameters such as Reynolds number or Froude number of individual phases. There is no well-defined transition boundaries between individual flow patterns because the transition of the flow patterns from one to another is gradual. This present study will make use of (Shoham, 2006) flow pattern map, but a concise discussion about different flow pattern maps from different researchers is presented in this section.

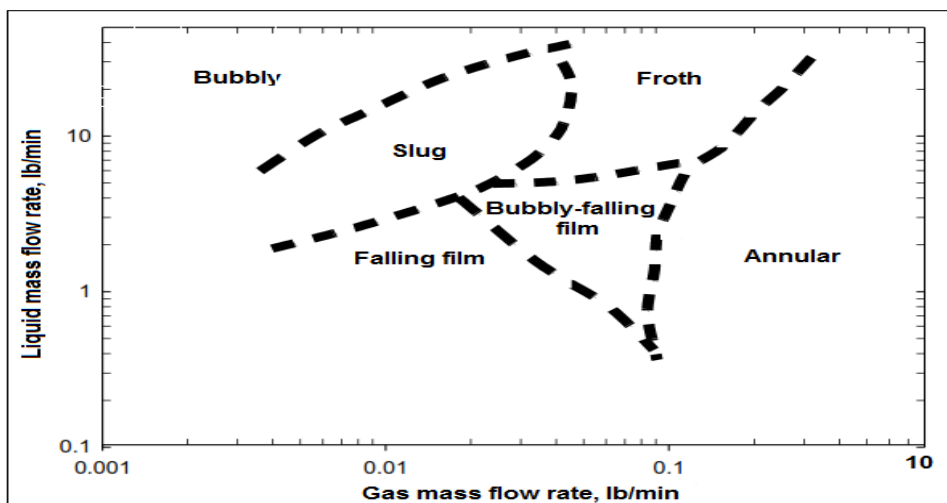


**Fig 2.3:** (Oshinowo, 1972) vertical downward flow pattern map (adapted from (Almabrok, 2013))

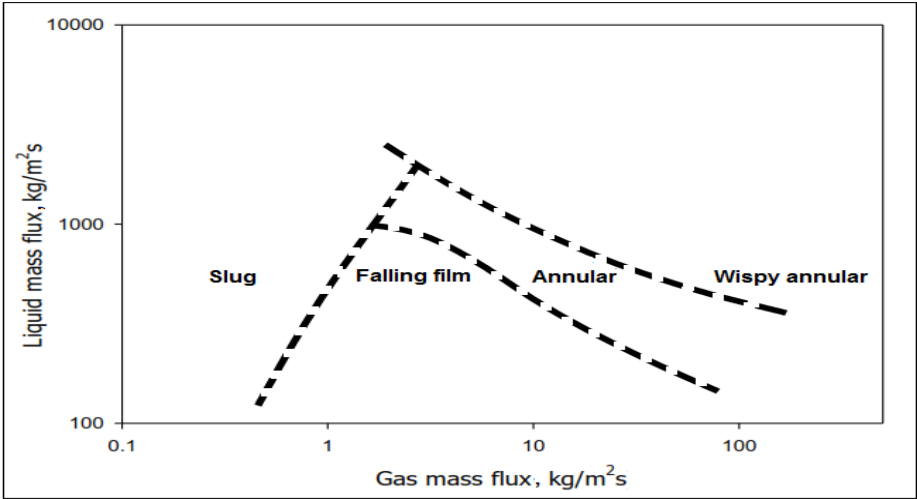


Fig 2.4: (Yamazaki & Yamaguchi, 1979) flow pattern map for vertical flow

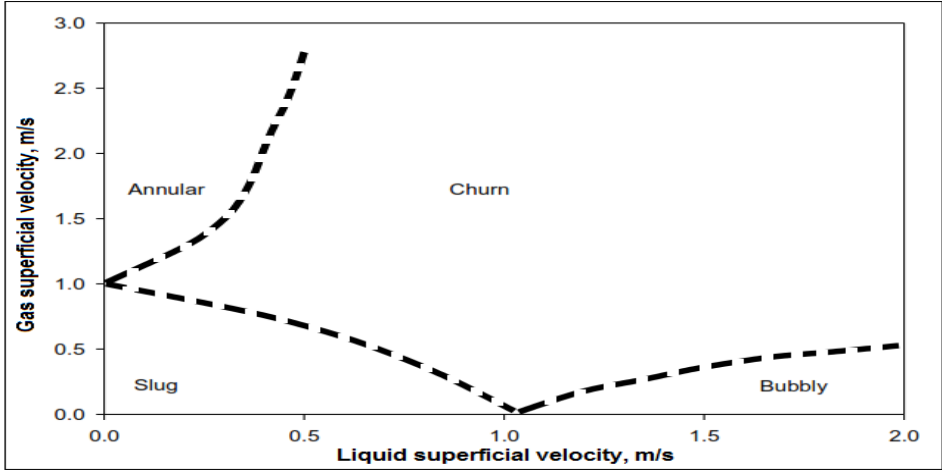
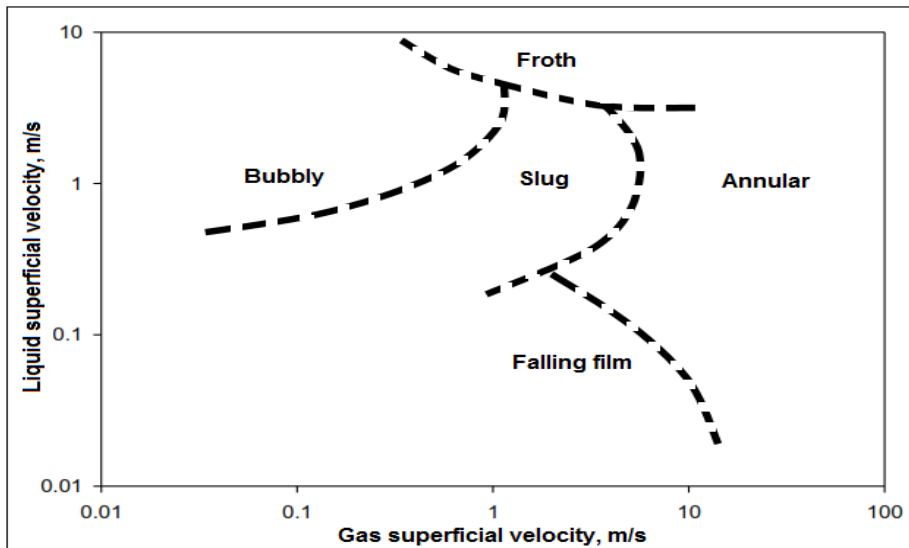


Fig 2.5: (Paras, 1982) vertical flow pattern map (adapted from (Almabrok, 2013))



**Fig 2.6:** (Yijun & Rezkallah, 1993) flow pattern map (adapted from (Almabrok, 2013))

## 2.4 Void Fraction and Liquid Hold Up

### 2.4.1 Liquid hold up:

Liquid hold up,  $H_L$ : In order to calculate quantities like density, actual gas and liquid viscosities, effective viscosity and heat transfer the knowledge of liquid hold up is very important.

Liquid hold up can be defined as the fraction of an element of pipe which is occupied by liquid at the same instant. Its value varies from zero for single phase gas to one for single phase liquid phase.

$$H_L = \frac{\text{volume of liquid in pipe element}}{\text{volume of pipe element}}$$

It can be determined experimentally by using methods like; resistivity or capacitance probes or by trapping segment of the flow stream between quick closing valves and measuring the volume of liquid trapped. For mixture of gas and liquid, gas hold up known as void fraction,  $H_g$  can be expressed as;

$$H_g + H_L = 1$$

Since the value of liquid hold up cannot be determined by analytic method, it is usually determined from empirical correlation which depends on variables such flow patterns, fluid properties, pipe diameter and angle of inclination. The equations that govern liquid hold up depend on dimensionless gas and liquid velocity numbers together with liquid viscosity number and angle of inclination. When there is slippage between the gas and liquid phase which result when gas and liquid flow concurrently in a pipe, the liquid travel slower than the gas and therefore the in-situ liquid volume fraction at any given cannot be computed directly from input conditions.

In two-phase flow, and accurate prediction of liquid hold up is needed to compute hydrostatic head losses. One of the attempts made to develop the empirical correlation of preceding liquid hold up is the liquid hold up of Hagedorn and Brown which was calculated but not measured to satisfy the pressure gradient that was measured after the pressure gradient due to friction and acceleration were put into account using data from 51 field pressure profiles of vertical well. (Duns Jr & Ros, 1963) also developed a correlation based on flow pattern map and function on the slip of velocity while Griffith develops correlation as a gas void fraction for bubble flow.

#### **2.4.2 Void fraction:**

To characterise two-phase flow in pipes the knowledge of void fraction is very important. The void fraction otherwise known as cross-sectional void fraction  $\mathcal{E}$  is a dimensionless geometric parameter which is defined as the ratio of the pipe cross-sectional area  $A_g$  occupied by the gas to the total cross-sectional area  $A$  of the pipe;

$$\mathcal{E} = \frac{A_g}{A} = \frac{A_g}{A_l + A_g}$$

The void fraction is a flow parameter bounded between 0 for single phase liquid flow and a for single phase gas flow. For void fraction close to 0<sup>+</sup> is a characteristic of bubbly two-phase flow with most of the cross-section of the pipe occupied by the liquid phase and only

few gas bubbles entrained in the continuous liquid phase while void fraction of 1 is a characteristic of dispersed mist flow with most of the cross-section of the pipe occupied by the gas and only a few liquid droplets entrained in the continuous gas phase.

In general, the void fraction is related to the morphology of the two-phase flow. Void fraction value below 0.2-0.3 is bubbly flow; about 0.2 - 0.3 to 0.7-0.8 is intermittent flow while above 0.7-0.8 is annular and mist flow.

In addition to the concept of cross-sectional void fraction  $\epsilon$ , void fraction can also be defined in terms of volumetric and chordal void fraction.

Volumetric void fraction  $\epsilon_v$  can be defined as the ratio of volume of the pipe occupied by the gas  $V_g$  to the total volume  $V$  of the pipe;

$$\epsilon_v = \frac{V_g}{V} = \frac{V_g}{V_l + V_g}$$

Chordal void fraction  $\epsilon_{ch}$  can be defined as the ration of the chord length lying in the gas  $L_g$  to the total length of the cord  $L$ ;

$$\epsilon_{ch} = \frac{L_g}{L} = \frac{L_g}{L_l + L_g}$$

In two phase flow, that compliment to void fraction is the liquid hold up i.e.  $H_L=1-\epsilon$

#### **2.4.3 Void fraction correlation:**

In contrast to exhaustive literature and void fraction correlations available for horizontal and vertical upward flow, little research has been done so far for downward two phase flow. The void fraction correlations available in literature can be classified in terms of the method and physics involved in deriving these correlations. Further they can be subcategorized as flow dependent, flow independent and correlations not developed for but applicable to downward two phase flow. The literature search in this work showed that most of the correlations

available for downward two phase flow are flow pattern dependent designed typically for concept based on drift flux model.

Authors	Correlation
(Clark & Flemmer, 1985)	$\varepsilon = \frac{U_{SG}}{1.17U_M \pm 1.53 \left( \frac{g\sigma\Delta\rho}{\rho_l^2} \right)^{0.25}}$
(Dix, 1971)	$\varepsilon = \frac{U_{SG}}{\frac{U_{SG}}{U_M} \left[ 1 + \left( \frac{U_{SL}}{U_{SG}} \right)^{\left( \frac{\rho_g}{\rho_l} \right)^{0.1}} \right] U_M \pm 2.9 \left( \frac{g\sigma\Delta\rho}{\rho_l^2} \right)^{0.25}}$
(Cai, Chen, & Ye, 1997) <b>(bubbly flow)</b>	$\varepsilon = \frac{U_{SG}}{1.185U_M \pm 1.53 \left( \frac{g\sigma\Delta\rho}{\rho_l^2} \right)^{0.25}}$
(Cai et al., 1997) <b>(slug flow)</b>	$\varepsilon = \frac{U_{SG}}{1.15U_M \pm 0.345 \sqrt{gD \left( \frac{\Delta\rho}{\rho_l} \right)}}$
(Gomez, Shoham, Schmidt, Chokshi, & Northug, 2000)	$\varepsilon = \frac{U_{SG}}{1.15U_M + 1.53 \left( \frac{g\sigma\Delta\rho}{\rho_l^2} \right)^{0.25} (1 - \varepsilon)^{0.5} \sin \theta}$
(Greskovich & Cooper, 1975)	$\varepsilon = \frac{U_{SG}}{1.0U_M \pm 0.671 \sqrt{gD(\sin \theta)^{0.263}}}$
(Hasan, 1995)	$\varepsilon = \frac{U_{SG}}{1.12 \pm 0.345 \sqrt{gD \left( \frac{\Delta\rho}{\rho_l} \right)}}$
(Kokal & Stanislav, 1989)	$\varepsilon = \frac{U_{SG}}{1.2U_M \pm 0.345 \sqrt{gD \left( \frac{\Delta\rho}{\rho_l} \right)}}$
(Nicklin, Wilkes, & Davidson, 1962)	$\varepsilon = \frac{U_{SG}}{1.2U_M \pm 0.35 \sqrt{gD}}$
(Woldesemayat & Ghajar, 2007)	$\varepsilon = \frac{U_{SG}}{\frac{U_{SG}}{U_M} \left[ 1 + \left( \frac{U_{SL}}{U_{SG}} \right)^{\left( \frac{\rho_g}{\rho_l} \right)^{0.1}} \right] U_M \pm 2.9(1.22 + 1.22 \sin \theta)^{\frac{P_{atm}}{P_{sys}}} \left( g\sigma D(1 + \cos \theta) \left( \frac{\Delta\rho}{\rho_l^2} \right) \right)^{0.25}}$

Table 2.1: 10 top performing correlations for vertical downward and upward two-phase flow (Bhagwat & Ghajar, 2012a) based on concept of drift-flux

#### 2.4.4 Void fraction correlation based on momentum balance:

(Usui & Sato, 1989) developed a simpler method to predict void fraction in falling film/annular flow regime for small pipes which can be also checked in large diameter pipes. The equation

used two parameters the wall friction factor ( $C_w$ ) which has a value of 0.005 and liquid

Froude number ( $F_{rf}$ ) defined by;

$$F_{rf} = \frac{U_{SL}}{\sqrt{gD \frac{\Delta\rho}{\rho_l}}} \dots \dots \dots (2.1)$$

The void fraction can therefore be predicted by;

$$\varepsilon = 1 - (2C_w F_{rf}^2)^{\frac{7}{23}} \dots \dots \dots (2.2)$$

#### 2.4.5 Drift Flux Model constitutive equations:

The important ingredients of drift flux model are the distribution parameter  $C_o$  and the drift velocity  $U_{GM}$ . The constitutive equations developed by different researchers for vertical upward and downward two-phase flow to determine the drift velocity and distribution parameters will be discussed here for large pipes:

Author(s)	Distribution parameter	Drift velocity
(Goda, Hibiki, Kim, Ishii, & Uhle, 2003) <b>(annular flow)</b>	$C_o = 1.2 - 0.2 \left( \sqrt{\frac{\rho_g}{\rho_l}} \right)$	$U_{GM} = 3 \left( \sqrt[4]{\frac{\sigma g \Delta\rho}{\rho_l^2}} \right)$
<b>Comination of Clark-Flemmer and Hirao (churn regime)</b>	$C_o = 0.934(1 + 1.42\langle\varepsilon\rangle)$	$U_{GM} = 1.53 \left( \sqrt[4]{\frac{\sigma g}{\rho_l}} \right)$
<b>Godal et al, 2003</b>	$C_o = (-0.0214\langle Um^* \rangle + 0.772) + (0.0214\langle Um^* \rangle + 0.228) \sqrt{\frac{\rho_g}{\rho_l}}$ For $-20 \leq \langle Um^* \rangle < 0$	$U_{GM} = \sqrt{2} \left( \sqrt[4]{\frac{\sigma g \Delta\rho}{\rho_l^2}} \right)$
(Haramathy, 1960)		$U_{GM} = 1.53 \left( \sqrt[4]{\frac{\sigma g \Delta\rho}{\rho_l^2}} \right)$
(Hirao, Kawanishi, Tsuge, & Kohriyama, 1986)	$C_o = 0.9 + 0.1 \sqrt{\frac{\rho_g}{\rho_l}}$	$U_{GM} = \sqrt{2} \left( \sqrt[4]{\frac{\sigma g \Delta\rho}{\rho_l^2}} \right)$

(Kataoka & Ishii, 1987)	$C_o = 1.2 - 0.2 \sqrt{\frac{\rho_g}{\rho_l}}$	$U_{GM} = U_{GM}^+ \left( \sqrt[4]{\frac{\sigma g \Delta \rho}{\rho_l^2}} \right)$ $U_{GM}^+ = 0.92 \left( \frac{\rho_g}{\rho_l} \right)^{-0.157} \text{ for } D_H^* \geq 30$ $N_{\mu l} = \frac{\mu_l}{\sqrt{\rho_l \sigma \sqrt{\frac{\sigma}{g \Delta \rho}}}}$
(Kawanishi, Hirao, & Tsuge, 1990)	$C_o = 0.9 + 0.1 \sqrt{\frac{\rho_g}{\rho_l}} \text{ for } -2.5 \leq \langle U_M \rangle < 0$	$U_{GM} = \sqrt{2} \left( \sqrt[4]{\frac{\sigma g \Delta \rho}{\rho_l^2}} \right)$
(Ishii, 1977) (churn flow)	$C_o = 1.2 - 0.2 \sqrt{\frac{\rho_g}{\rho_l}}$	$U_{GM} = \sqrt{2} \left( \sqrt[4]{\frac{\sigma g \Delta \rho}{\rho_l^2}} \right)$
(Clark & Flemmer, 1985)	$C_o = 0.93 \frac{\langle U_{SL} \rangle}{\langle U_M \rangle} + 1.95 \frac{\langle U_{SG} \rangle}{\langle U_M \rangle}$	$U_{GM} = 0.25$

**Table 2.2:** constitution equation for drift-flux related to large diameter pipes

## 2.5 Power Spectrum Density (PSD):

The power spectrum density approach is obtained by performing Fourier transform auto covariance functions of the time series of cross-sectional averaged void fraction to obtain the frequency characteristics of the time series (Abdulkadir, Mbalisigwe, Zhao, Azzopardi, & Tahir, 2019). The dominant frequency obtained corresponds to the frequency at the peak of the variation of PSD with frequency (Sharaf, van der Meulen, Agunlejika, & Azzopardi, 2016).

The Fourier transform of time series signal is first carried out to obtain the PSD and it is given by (Kanu, 2013) as;

$$F(x) = \int_{-\infty}^{\infty} \varepsilon_l(t) e^{(-2\pi f t) dt}$$

PSD is obtained by taking the Fourier transform of the auto covariance (ACF) (Kanu, 2013)

$$C_{xx}(k'\tau) = \frac{1}{t-\tau} \int_0^{t-\tau} (\varepsilon_l(t) - \varepsilon_l') (\varepsilon_l(t+k'\tau) - \varepsilon_l') dt, \quad \tau < T$$

Where T= sampling duration  $\tau =$  interrogating decay time  $k\Delta\tau =$  time decay

PSD is given by;

$$P_{xx}(f) = \tau \left( \frac{1}{2} C_{xx}(0) + \sum_{k=1}^{\frac{t}{\tau}-1} C_{xx}(k'\tau) \omega(k'\tau) \cos(2\pi f k'\tau) \right)$$

A cosine window function  $\omega(k\Delta\tau)$  is used to suppress the leakage in the spectrum (adapted from (Abdulkadir et al., 2019)).

## CHAPTER THREE

### METHODOLOGY

#### 3.1 Data Acquisition:

The present experimental programme was carried out in a large close loop facility located within the Chemical Engineering Laboratories of the University of Nottingham United Kingdom. The whole set up made use of air-water fluid combination using 127mm diameter pipe of 90° and -90° vertical pipe orientations. The cross-sectional film fractions as a function of time was measured using conductance ring probes. The probes were constructed by mounting two stainless plates separated by a spacer between a pair of thick acrylic blocks and machining a hole through them so that they can flush the pipe inner wall placed at specified distances above the mixer section is the probe 1 for upward flow and probe 4 for downward flow.

#### 3.2 Data Processing:

The void fraction as a function of time at two locations when the pipe is at 90° and -90° for 15000 data points obtained from the conductance ring probe method were processed for 17 different runs for 16 L/min to 150l/min of liquid superficial velocity which is later converted to the S.I unit at the range of gas superficial velocity of (3.45-10.05) m/s. spectral analysis was conducted using the power spectrum density (PSD) which uses the Fourier transform auto covariance of time series. The void fractions for 15000 data points for the 17 runs at the two probes for riser and down comer were inserted into the PSD Macro templates using a sampling frequency of 1000 Hertz. After the macro was ran the dominant frequency was obtained for each liquid superficial velocity for the 17 runs. The averaged void fraction were obtained for the liquid superficial velocities in both orientations and tabulated to obtain the gas actual velocity ( $V_G$ ) and the mixture velocity ( $U_M$ ) for corresponding gas superficial velocities by using the simple relation below;

$$V_G = \frac{U_{SG}}{\epsilon} \dots \dots \dots (3.1)$$

$$U_M = U_{SL} + U_{SG} \dots \dots \dots (3.2)$$

**3.3 Data Analysis:**

The plot of average void fraction against the gas superficial velocity (3.45-10.05)m/s at liquid superficial velocity of (0.02-0.2)m/s was done for the two orientations. The dominant frequencies were plotted against the gas superficial velocity and a relationship will be established for the two orientations. The comparison of the cross-section of the averaged void fraction was done by using existing correlations and the experimented values for vertical upward and downward flows.

**3.4 Identification of Downward Flow Regime:**

One of the simplest ways to determine a flow regime is by the use of flow pattern maps. This work used the (Shoham, 2006) semi- mechanistic model of plot of  $U_{SL}$  against  $U_{SG}$  plot of the dataset by setting the fluid properties, the pipe geometry and the interfacial boundary of the phases, after which the model was run to determine the flow regimes of the experimental dataset for the upward and downward air-water flow. The flow regime was also identified using Probability density function (PDF) analysis and time series analysis.

**3.5 1-D Drift Flux Model:**

To predict the void fraction in gas-liquid two-phase flow is to use (Zuber & Findlay, 1965) one dimensional drift flux model. Using the drift flux model, a plot of actual velocity  $U_G$  against mixture velocity  $U_M$  will give a linear function with a high coefficient of correlation. The drift parameters,  $C_0$ , and drift velocity  $U_{GM}$  will be determined as the slope and intercept of the graphs respectively. These plots will be for the individual flow regimes to account for the different conditions governing the transition of each of the flow regimes. The equation that will be employed for the model generation is given by:

$$\epsilon = \frac{U_{SG}}{C_0 U_M \pm U_{GM}} \dots \dots \dots (3.3)$$

By rearranging the equation above;

$$\frac{U_{sg}}{\varepsilon} = U_G = C_o U_M \pm U_{GM} \dots \dots \dots (3.4)$$

### 3.6 Analysis of Performance of Void Fraction Correlations and Validation Of Co and U<sub>GM</sub> Constitutive Equations:

The performance 10 out of the 17 top performing correlations based on drift-flux model identified by (Bhagwat & Ghajar, 2012a) and the one identified by (Wang, Li, Yang, et al., 2018) to predict flow in annular/falling film which is based on the concept of momentum equation were used to predict the void fractions for (0.02-0.2) m/s and (3.45-10.05)m/s of U<sub>SG</sub> and U<sub>SL</sub> respectively for the Upward and Downward two-phase flow. The predicted void fractions were compared to those obtained experimentally to identify the one that best predict the void fraction in both orientations. The error and the RMS error were calculated and cross plot of the void fraction of both the past works and present work was done.

Different constitutive equations developed by top researchers to predict the Co and U<sub>GM</sub> to validate how best they agree with the one obtained from the empirical correlation obtained in this work was looked out for. The percentage error and RMS error was also calculated in this case and the RMS error equation is presented below:

$$RMS\ error = \sqrt{\frac{1}{N-1} \sum_{i=1}^n \left( \frac{\varepsilon_{measured} - \varepsilon_{predicted}}{\varepsilon_{measured}} \right)^2} \times 100 \dots \dots \dots (3.6.1)$$

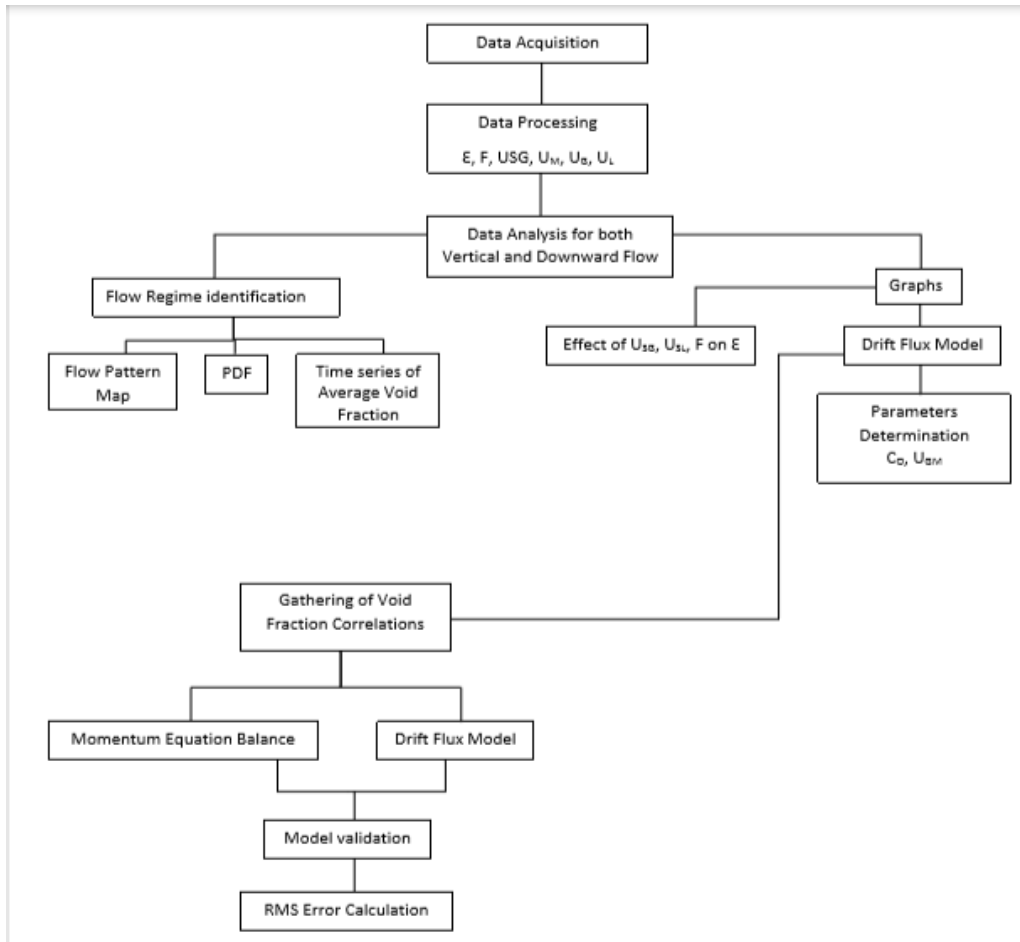


**Fig 3.1:** Flow chart of the Methods

## CHAPTER FOUR

### Results and Discussion:

The Air-water flow presented here for upward and downward flow in 127mm pipe are in the range of 3.45m/s to 16.05 m/s and 0.02 to 0.2m/s for gas superficial velocities and liquid superficial velocities respectively.

Table 4.1: Physical properties of air-water at test conditions

$\rho_{\text{air}}$	$\rho_{\text{water}}$	$\sigma_{\text{air-water}}$	$P_{\text{system}}$	$P_{\text{atm}}$	$T$	$\mu_{\text{water}}$
3.55kg/m <sup>3</sup>	998kg/m <sup>3</sup>	0.072N/m	3bar	1.013bar	25 <sup>0</sup> C	1cp (10 <sup>-3</sup> Pa.s)

### 4.1 Time Series of Void Fraction:

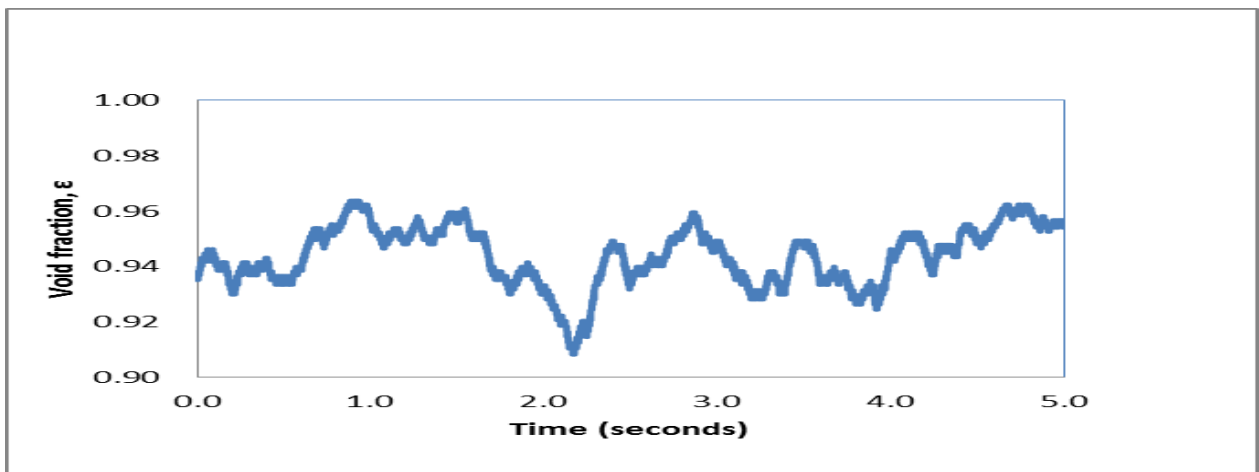


Fig 4.1(a): Time series for air-water flow for vertical upward at  $U_{\text{SL}}$  of 0.08m/s and  $U_{\text{SG}}$  of 9.92m/s

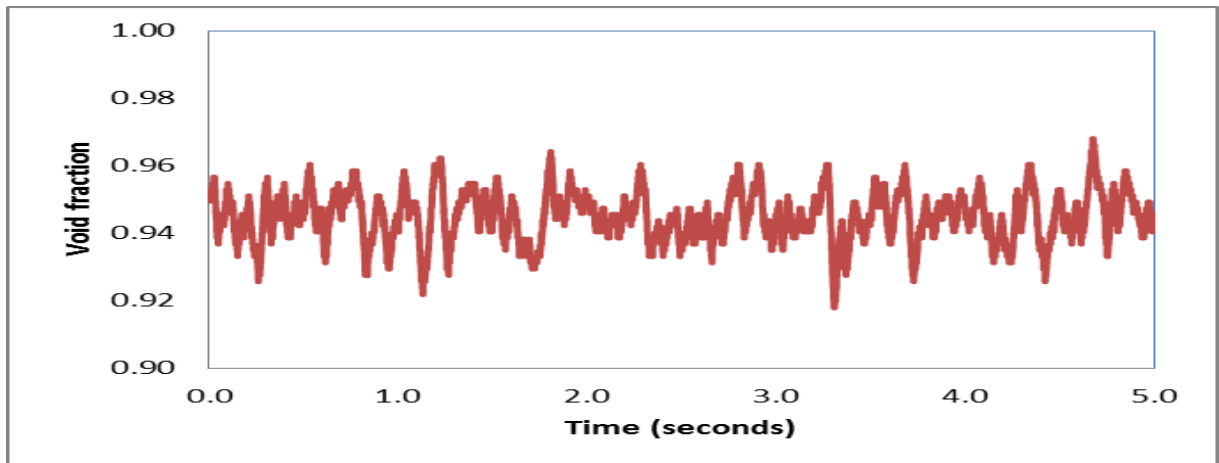


Fig 4.1(b): Time series for air-water flow in vertical downward at  $U_{SL}$  of 0.08m/s and  $U_{SG}$  of 9.92m/s

The plot of averaged void fraction data against time gives rise to the typical time series plots that are presented in Figs. 4.1(a) and 4.1(b) for upward and downward flow respectively.

(Costigan & Whalley, 1997) reported from their work that when many bubbles or void fractions are below 0.8 or when there are no low void fraction slugs remaining that Churn flow exist and that annular flow exists if all void fractions are above 0.8. From Figs. 4.1(a) and 4.1(b), it can be observed that there exists a high void fraction with regular troughs which peak at 0.96 which is in agreement with the report of (Costigan & Whalley, 1997).

(Bouyahiaoui, Azzi, Saidj, & Zeghloul, 2008) also explain the behaviour of churn turbulent to be similar to that of annular flow by visually observing the chaotic nature of both regimes which makes it difficult to distinguish it from annular flow as it is observed by most studies. But since the void fraction value is above 0.8 it is therefore right to say the flow is annular. There exists a minor difference from the time series plot for all the range of data for liquid and gas superficial velocities as it was also observed by (Abdulkadir et al., 2019).

Other methods for identifying flow pattern will be looked at because time series alone cannot be used to justify flow patterns. These other methods will be discussed in the subsequent sections.

#### 4.2 Probability Density Function (PDF):

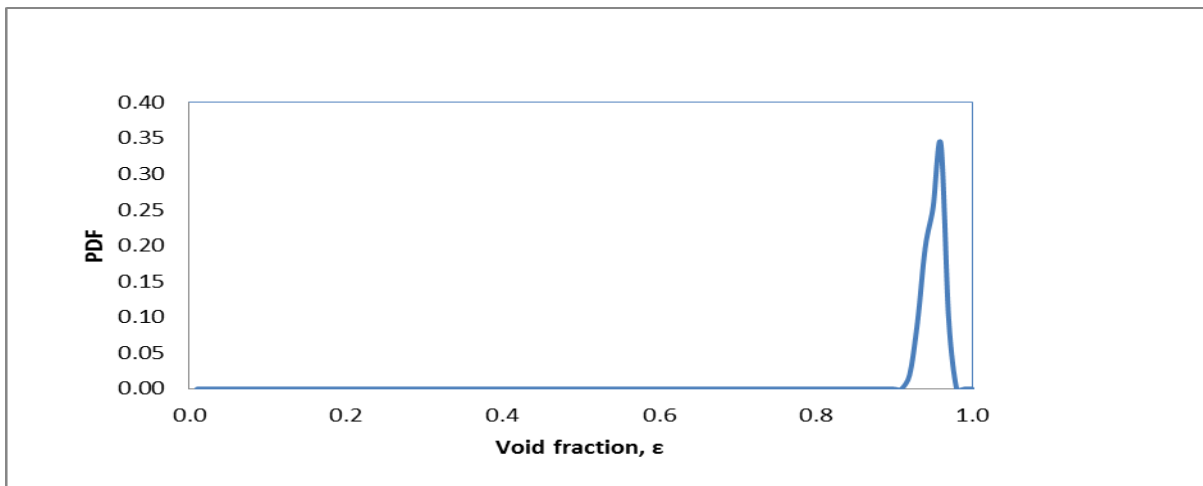


Fig 4.2a: PDF for air-water flow in vertical upward at  $U_{SL}$  of 0.08m/s and  $U_{SG}$  of 9.92m/s

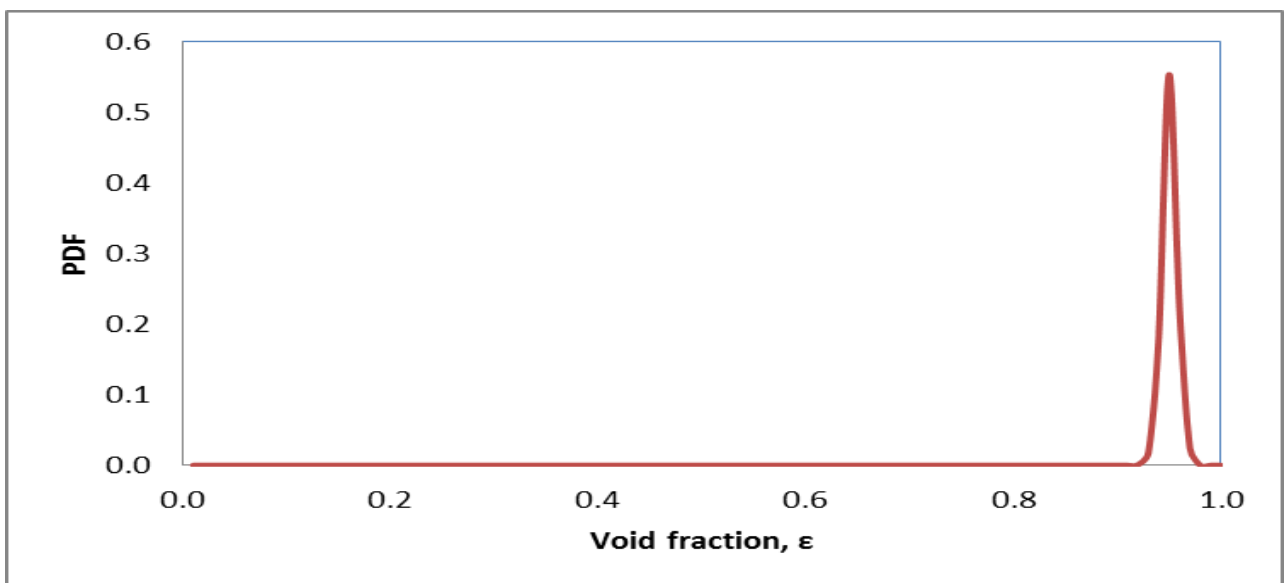


Fig 4.2b: PDF for air-water flow in vertical downward at  $U_{SL}$  of 0.08m/s and  $U_{SG}$  of 9.92m/s

One can identify flow regimes by using the probability density function (PDF) through amplitude variation of the frequency of occurrence of each void fraction. Several literatures have reported two types of flow with the similar behaviour quantitatively which is the falling film which only occurs in vertical downward two-phase flow and annular flow. They explain the qualitative distinction between the two as one (annular) to be more chaotic and turbulent than the other (falling film). The PDF distribution for the vertical upward and the downward

flow are characterised by a single narrow peak as compared to churn-turbulent flow with a single peak that is wide and flat at which follows the trend reported by (Hernandez Perez, V. and Azzopardi, 2018), (Omebere-Iyari & Azzopardi, 2007) using a 189mm diameter pipe, (Yang et al., 2018) of pipe diameter 152.4mm and (Wang, Li, Yang, et al., 2018) of 203.2mm diameter pipe.

For all the data points analysed for upward and downward flow of 0.02- 0.2m/s and 3.45- 16.01m/s for the liquid and gas superficial velocities respectively. Single narrow pick can be observed at a very high void fraction which is closer to value of 1 which suggests the follow can be either falling film/annular as in the case of down flow and annular in the case of up flow. (Yang et al., 2018) of pipe diameter 152.4mm and (Yang et al., 2018) of 203.2mm diameter pipe reported that the structure of churn turbulent flow is chaotic and its PDF profile is scattered and has an averaged void fraction value( $\epsilon > 0.5$ ). Annular flow has a large void fraction peak and is characterised by a gas core occupying the centre of the pipe surrounded by continuous liquid film passing through the pipe wall. Since the falling film does not have a disturbed time series it is therefore right to say the trend signifies the flow is in the annular regime occurring at very high void fraction in both pipe orientations.

### 4.3 Flow pattern Map:

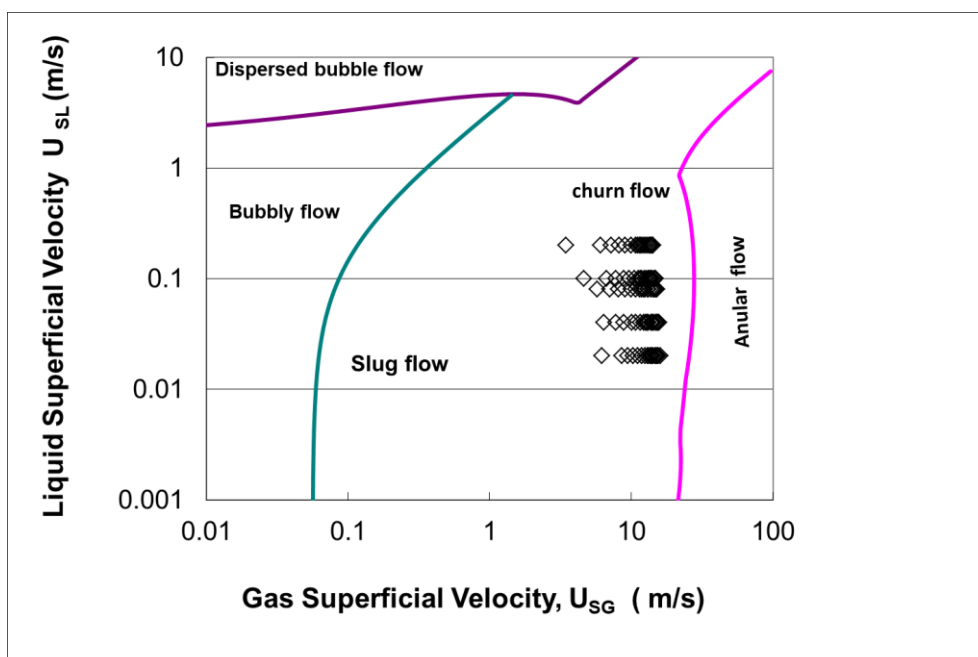


Fig 4.3a: Flow pattern map for vertical upward flow

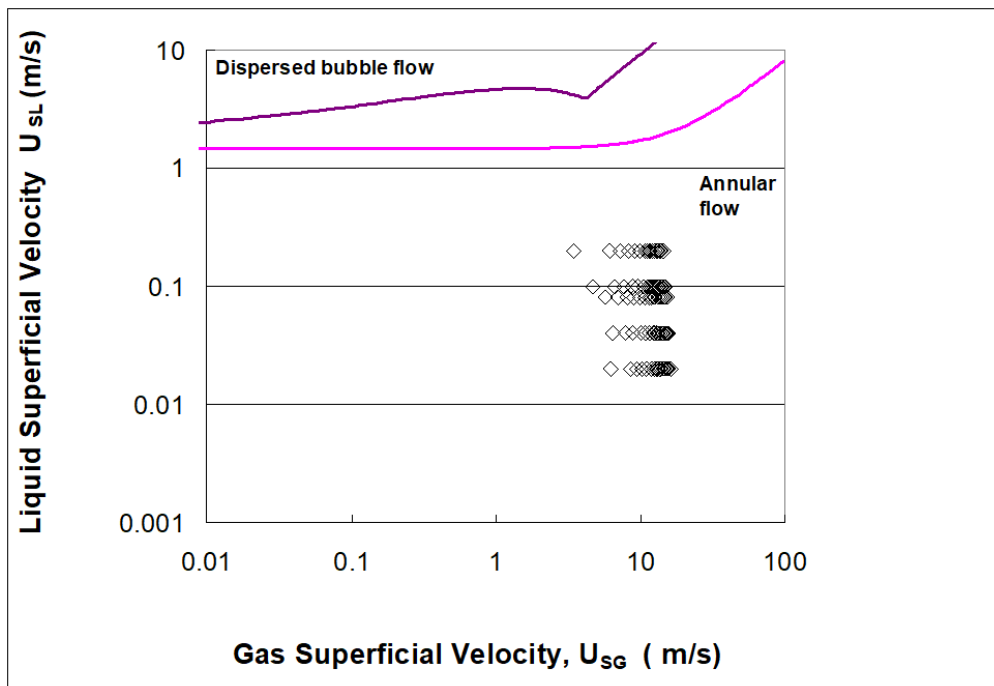
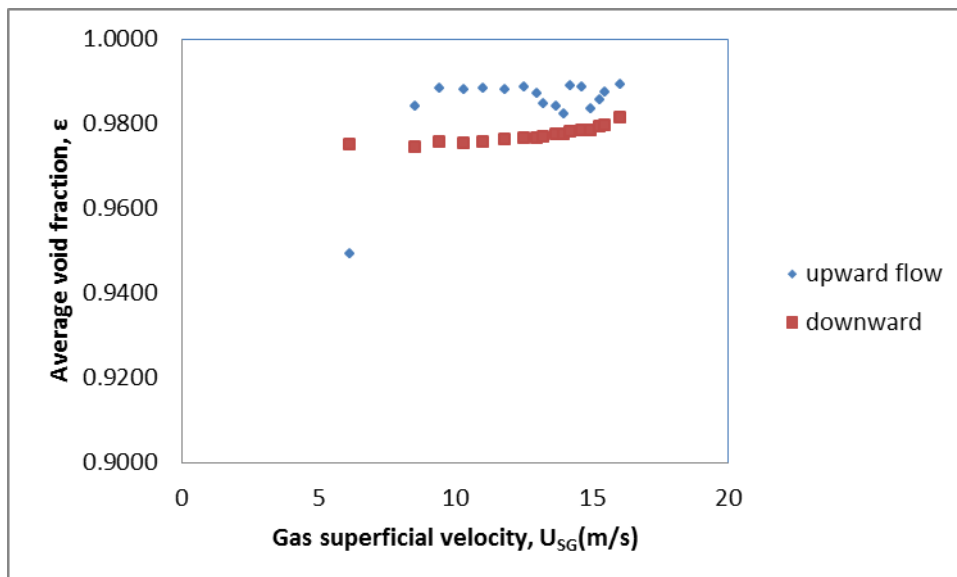
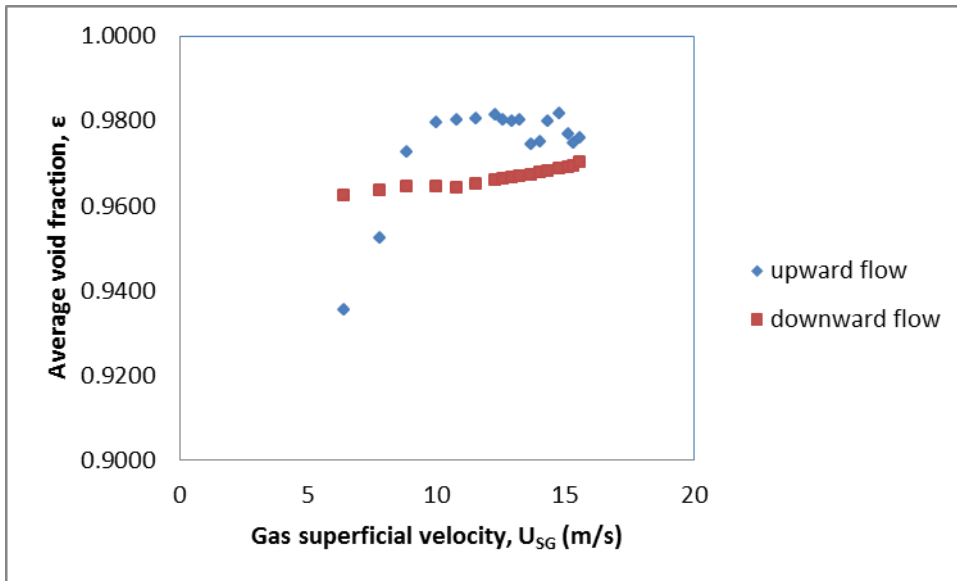


Fig 4.3b: Flow pattern map for vertical downward flow

#### 4.4 Variation of Averaged Void Fraction on Liquid and Gas Superficial Velocity:



**Fig 4.4a:** plot of average void fraction versus gas superficial velocity at  $U_{SL}$  of 0.02m/s



**Fig 4.4b:** plot of average void fraction versus gas superficial velocity at  $U_{SL}$  of 0.04m/s

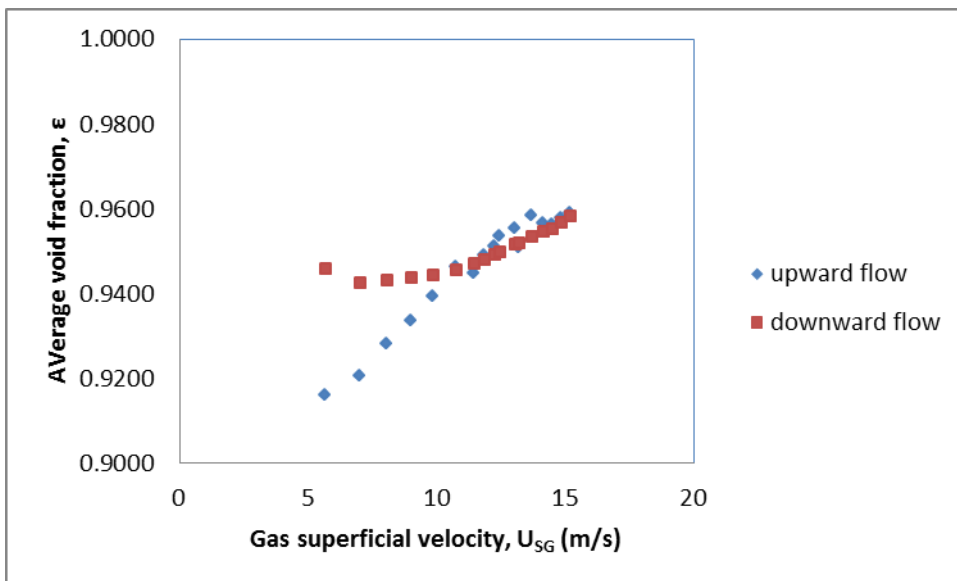


**Fig 4.4c:** plot of average void fraction versus gas superficial velocity at  $U_{SL}$  of 0.08m/s

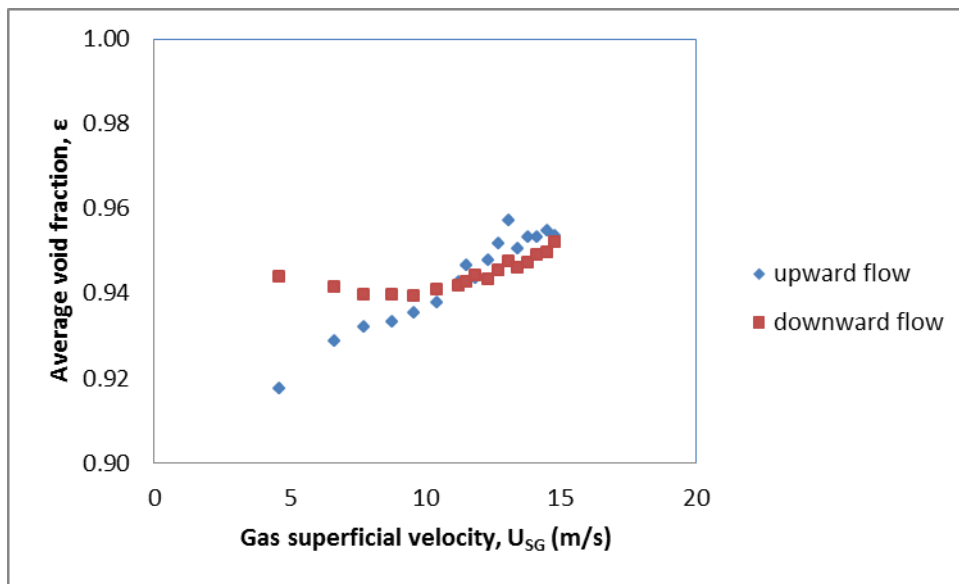


**Fig 4.4d:** plot of average void fraction versus gas superficial velocity at  $U_{SL}$  of 0.1m/s

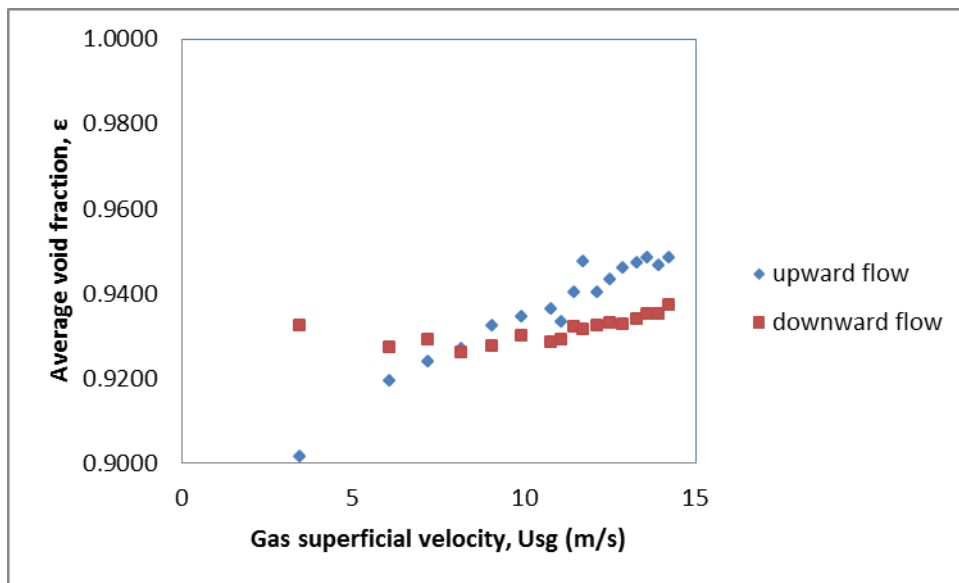


**Fig 4.4e:** plot of average void fraction versus gas superficial velocity at  $U_{SL}$  of 0.2m/s

From the figs 4.4 (a-e) the average void fractions were plotted against the gas superficial velocity from the data obtained from (0.02-0.2) m/s and (3.45-16.01) m/s of the liquid and gas superficial velocities respectively. It can be seen that void fraction depends on both gas and liquid superficial velocities. It can be observed in general that the average void fraction increases with gas superficial velocity and become lower with increase in liquid superficial velocity. The same trend was observed in Bhagwat et al (2012) in 12.7mm diameter pipe for

both vertical upward and downward two phase flow, (Godbole, Tang, & Ghajar, 2011) and (Omebere-Iyari & Azzopardi, 2007). As reported in the work of (Abdulkadir et al., 2019) an opposite trend was observed for the same data because they plotted average liquid film fraction (1- average void fraction) against gas superficial velocity in an upward flow.

From fig 4.4a with  $U_{SL}$  of 0.02m/s in the vertical upward flow the average void fraction increases rapidly at 0.94 with increasing gas superficial velocity until it become steady and reaches minimum at  $U_{SG}$  of 15m/s before it starts to increase with the gas superficial velocity while in the vertical downward flow the average void fraction increases steadily with increasing gas superficial velocity.

From fig 4.4b with  $U_{SL}$  of 0.04m/s in the upward flow the average void fraction increases rapidly at 0.94 with increasing gas superficial velocity and become steady at some certain points until it reaches maximum at 15m/s before declining again with increasing gas superficial velocity while in the downward flow it increases steadily with increasing gas superficial velocity.

From fig 4.4c with  $U_{SL}$  of 0.08 m/s in the upward flow the average void fraction increases rapidly from 0.92 with increasing gas superficial velocity until it reaches maximum at  $U_{SG}$  of about 13m/s before declining while in the downward flow it decreases steadily with increasing gas superficial velocity before it starts to increase at  $U_{SG}$  of 10m/s gradually with the gas superficial velocity.

From fig 4.4d with  $U_{SL}$  of 0.1m/s in the upward flow the average void fraction increases rapidly from 0.92 with increasing gas superficial velocity until it reaches maximum at 13m/s before declining again while in the downward flow it first decline with increasing gas superficial velocity before rising gradually at  $U_{SG}$  of 10mls with increasing gas superficial velocity.

From fig 4.4e with  $U_{SL}$  of 0.2m/s in the upward flow the average void fraction increases rapidly from 0.9 with increasing gas superficial velocity and reaches minimum at 11m/s and reaches maximum again at 12m/s and finally decline with increasing gas superficial velocity

while in the downward flow it decline steady until it starts to increase at  $U_{SG}$  of 12m/s with increasing gas superficial velocity.

It can be seen from the trend that the average void fraction in the downward flow is greater than that of upward flow. (Bhagwat & Ghajar, 2012b) observed the same trend and explain the variation to be as a result of the actual gas velocity in the upward flow to be greater than that in the downward flow and vice-versa in terms of actual liquid velocity reason been the buoyancy force acting to reduce the actual gas velocity on downward flow while serving to increase the actual gas velocity in the upward flow. It can also be observed that the void fraction increases with an increase in gas superficial velocity and churn turbulent flow become more evident at the low gas superficial velocity of 3.5 m/s which shows good characteristics of churn flow features like oscillatory nature, large wave height and high film fraction with similar trend reported by previous investigators such as (Abdulkadir et al., 2019), (Almabrok, 2013) and (Wang, Li, Yang, et al., 2018). When the gas superficial velocity increases, the wave amplitude decreases which depicts good characteristics of annular flow.

(Abdulkadir et al., 2019) explain the decrease, increase and uniformity of void fraction with increase in  $U_{SG}$  to signify the smoothing of the interface and also thinning of the film, presence of liquid entrainment in the gas core which is as a consequence of bringing about thickness of film fraction and as a result of annular flow regime existing at higher  $U_{SG}$  respectively.

#### 4.5 Effect of Frequency on Gas and Liquid Superficial Velocity:

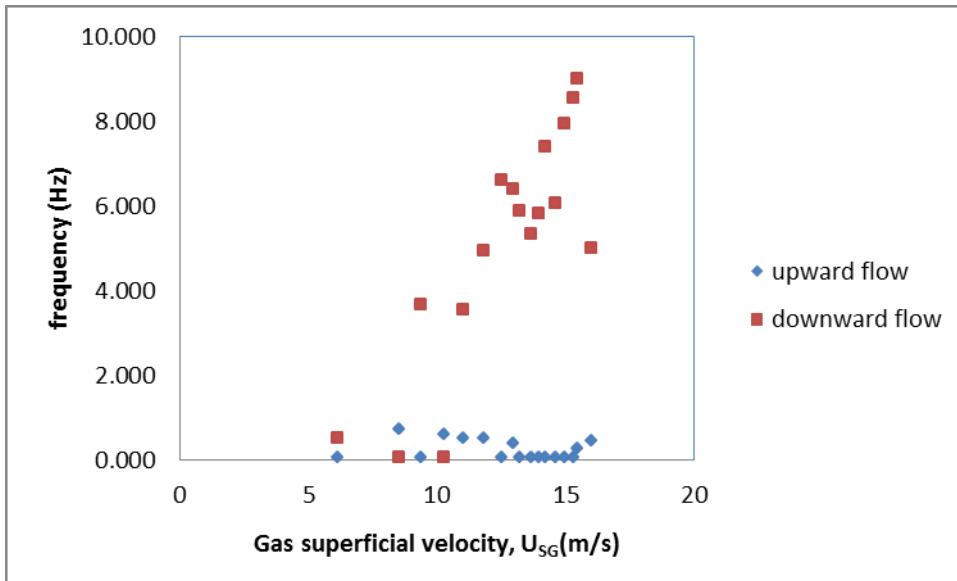
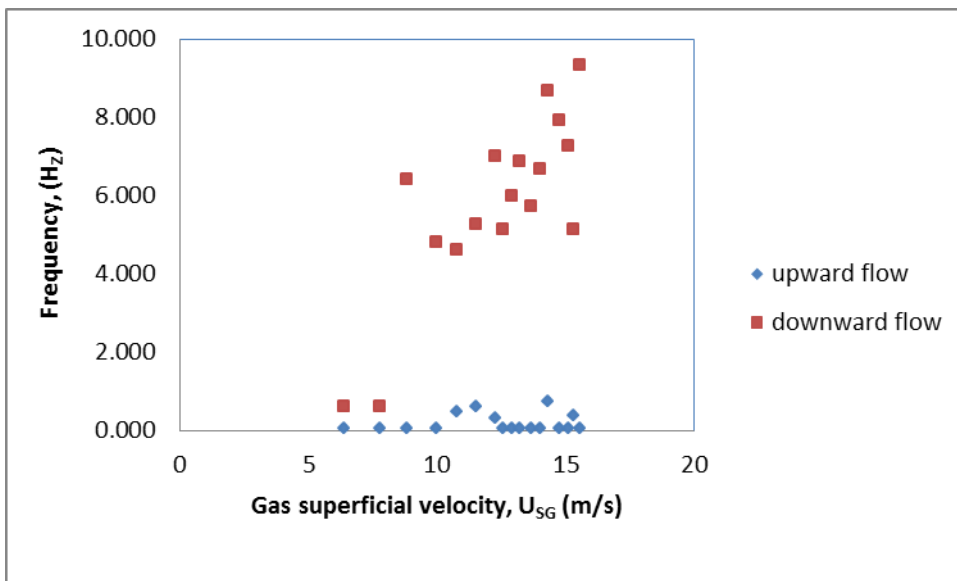
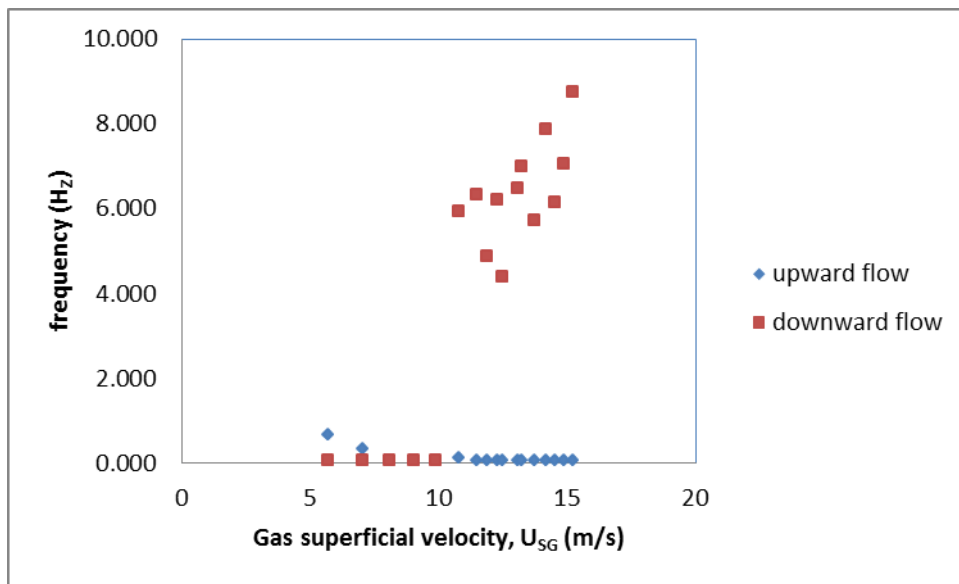


Fig 4.5a: plot of dominant frequency versus gas superficial velocity at  $USL=0.02\text{m/s}$



**Fig 4.5b:** plot of dominant frequency versus gas superficial velocity at  $USL=0.04\text{m/s}$



**Fig 4.5c:** plot of dominant frequency versus gas superficial velocity at  $USL=0.08\text{m/s}$

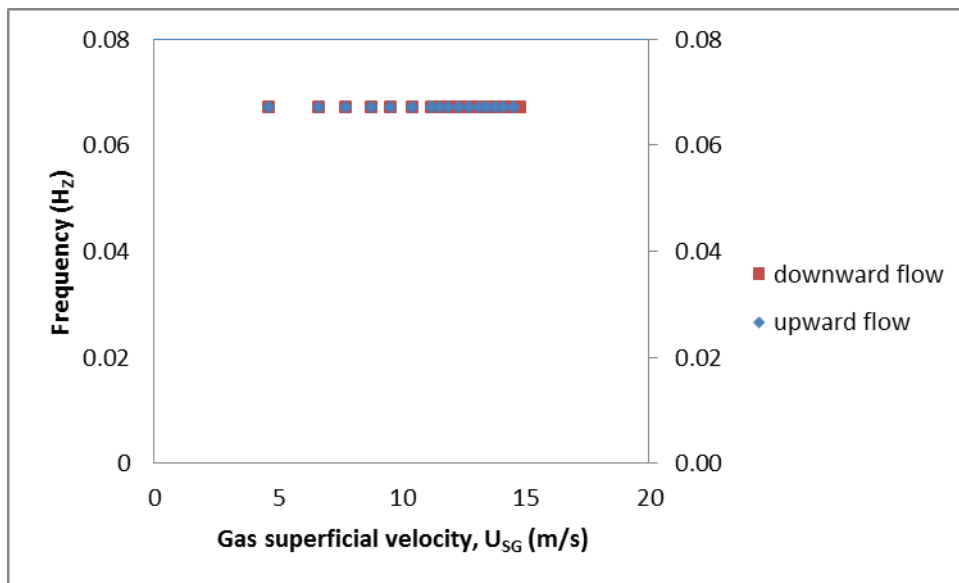


**Fig 4.5d:** plot of dominant frequency versus gas superficial velocity at  $U_{SL}=0.1\text{m/s}$

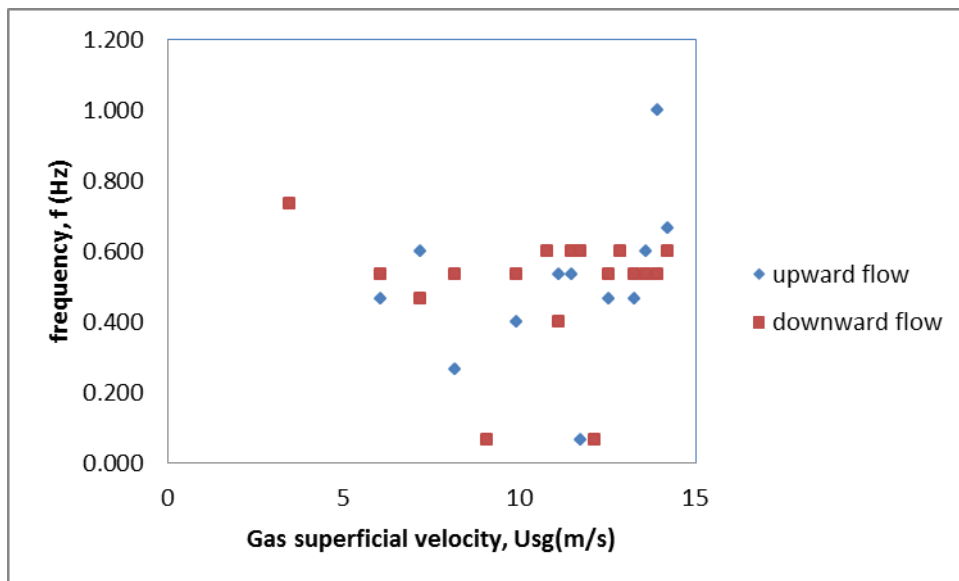


**Fig 4.5e:** plot of dominant frequency versus gas superficial velocity at  $U_{SL}=0.2\text{m/s}$

From the plot of data from the fig 4.4(a) to 4.4 (b) it can be observed that the frequencies are higher in the vertical downward flow than it is in the vertical upward flow but no significant difference in the frequencies at superficial velocities from 0.02 to 0.08m/s to about 10m/s and it becomes very low at higher liquid superficial velocity of 0.1 to 0.2m/s to about 0.07Hz. It can be seen from  $U_{SL}$  of 0.1 m/s for both upward and downward flow that the frequencies trend is constant with increasing gas superficial velocity but of the frequency at  $U_{SL}$  of 0.2m/s is more complex with no correlation between the upward and the downward flow. (Sharaf et al., 2016) reported similar trend for upward flow but in this work opposite trend can be observed for downward flow.

#### 4.6: Effect of Gas Actual Velocity on Mixture Velocity (Drift-Flux Model):

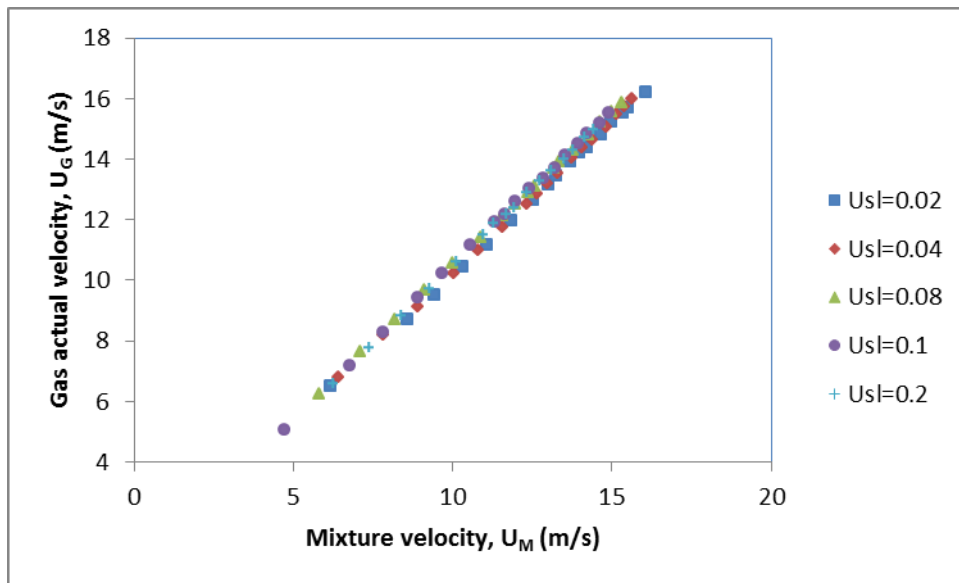


Fig 4.6(a): Drift-flux model for vertical downward flow

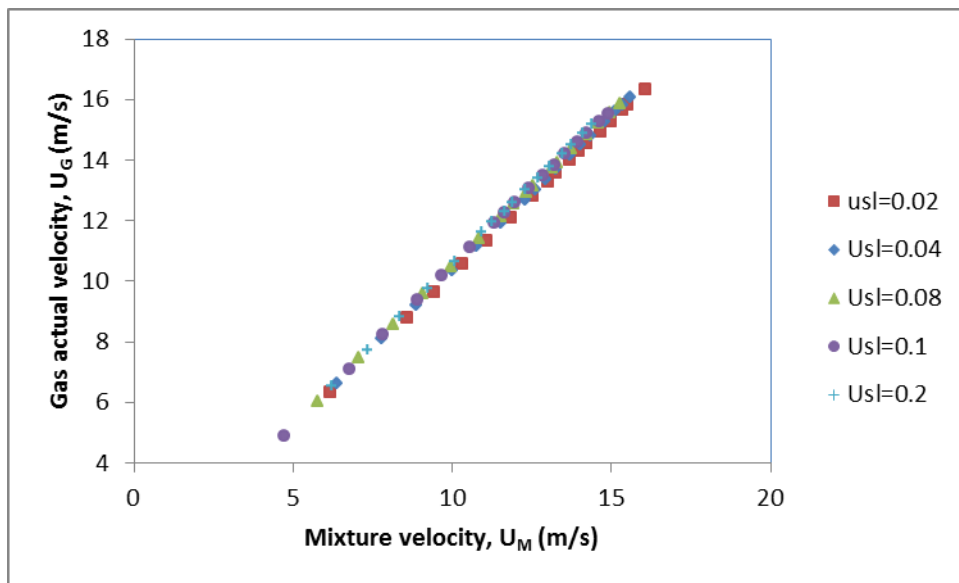


Fig 4.6(b): Drift-flux model for vertical upward flow

$U_{SL}$ (m/s)	upward flow		downward flow	
	$C_o$	$U_{GM}$ (m/s)	$C_o$	$U_{GM}$ (m/s)
<b>0.02</b>	1.0006	0.1569	1.0162	0.0646
<b>0.04</b>	1.0008	0.2551	1.0252	0.0686
<b>0.08</b>	1.0076	0.4607	1.0337	0.1329

0.1	1.0226	0.2846	1.0466	0.0261
0.2	1.0327	0.1327	1.0649	-0.126

**Table 4.2:** Distribution parameters and Drift velocity for Vertical upward and downward flows

From fig 4.4(a) and 4.5(b) it can be observed at the plot of gas actual velocity against mixture velocity at different liquid superficial velocity is a straight line for both upward and downward flow as it was proposed by (Zuber & Findlay, 1965) and adopted by different researchers. A positive slope can be observed in both figures as the gas actual velocity increases with increasing mixture velocity. From the linear plots the slope of the plots gives the drift velocity ( $U_{GM}$ ) while the intercept gives the distribution parameter ( $C_o$ ). Table 4.5 shows the distribution parameters and drift velocity for both upward and downward flow obtained from the equation of straight line for liquid superficial velocity of (0.02-0.2) m/s. looking at the trend from the table it can be seen that the distribution parameter is close to one for both orientation which flows the trend of (Bhagwat & Ghajar, 2012a) that defines  $C_o$  as the measure of the distribution of the gas phase with respect to the mixture across the pipe cross-section. They observed that the distribution parameter should change with flow patterns and pipe inclination. They assumed a value close to 1.2 for both vertical upward and downward flow but they observed that as the flow is moving towards regime of annular flow (where the liquid film is surrounded by gas core) the value of distribution parameter tends to unity. From the table for both pipe orientations  $C_o$  increases with increase in liquid superficial velocity which is almost constant and follows the trend of (Wang, Li, Yousaf, Yang, & Ishii, 2018) and (Sharaf et al., 2016).

(Bhagwat & Ghajar, 2012a) also explain the drift velocity to be the actual cross-sectional averaged velocity of the gas phase with respect to the averaged mixture velocity passing through the centre of the pipe. From table 4.5 the intercept of the linear graphs gives the  $U_{GM}$  that varies for the different liquid superficial velocity for both upward and downward flow except for the downward flow at  $U_{SL}$  of 0.02m/s that give a negative intercept which follow the statement made by (Bhagwat & Ghajar, 2012a) that the drift velocity for vertical

downward flow and upward flow can be used interchangeably by flipping the sign of the  $U_{GM}$  from positive to negative. (Wang, Li, Yousaf, et al., 2018) reported that the drift velocity increases with increase in liquid superficial velocity and that they are close to the absolute values of the corresponding inlet liquid superficial velocity that made them come to conclusion that drift velocity in annular flow regime depends on the inlet superficial velocity whereas in this work the  $U_{GM}$  increases with increase in  $U_{SL}$  from 0.02m/s to 0.08m/s until it starts to decline from 0.01m/s to 0.2m/s also there is no similarity between the inlet liquid superficial velocity and drift velocity in this work follows the trend of (Sharaf et al., 2016).

#### **4.7: Analysis of the Performance of Void Fraction Correlations:**

Since literatures do not provide clear and universal definition of flow patterns, correlation which is flow pattern dependent is used in this work to analyse all the data from 0.02 m/s to 0.2m/s of the superficial liquid velocity. By the analysis of 10 selected void fraction correlations that are based on drift-flux model available for vertical upward flow and the few available for downward two-phase flow. The momentum equation developed by (Usui & Sato, 1989) for falling film/annular is also adopted. Out of these 10 correlations the correlation of (Gomez et al., 2000) and (Nicklin et al., 1962) were mainly developed for upward flow while the correlation of (Cai et al., 1997), (Hasan, 1995) were developed for downward flow and (Woldesemayat & Ghajar, 2007) is developed for both orientations. The correlations were used for both pipe orientations by changing the sign of the drift velocity from positive to negative and vice versa. The analysis was important as these correlations were obtained for different pipe diameter, flow pattern, fluid combination and system pressure. The following was observed from the trend of the past works against the present study;

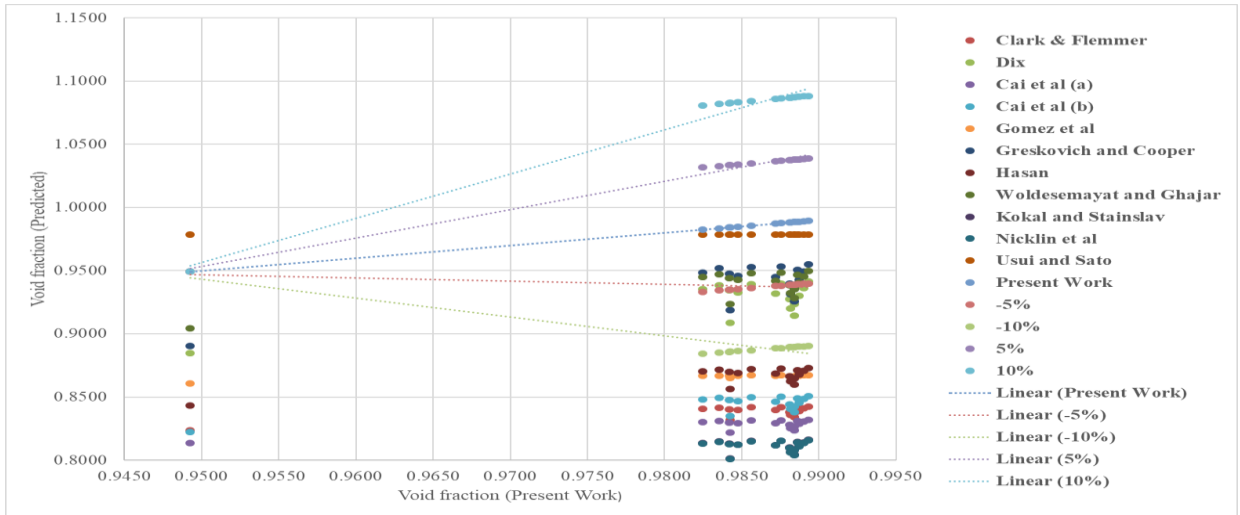


**Fig 4.7(a):** performance of 11 correlations for vertical upward air-water flow at  $U_{SL}$  of 0.02m/s

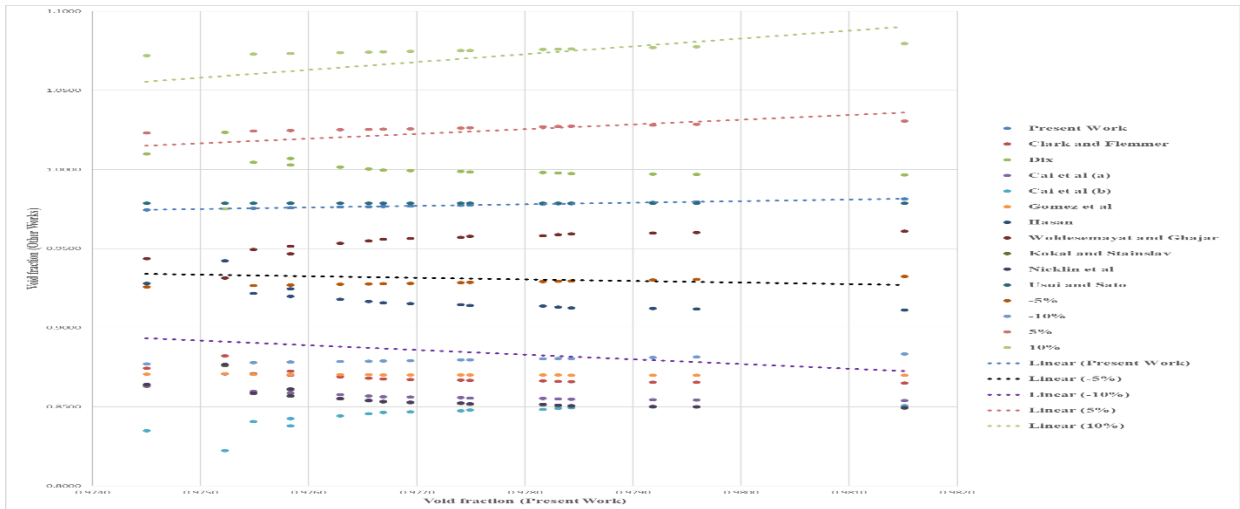


**Fig 4.7(b):** performance of 11 correlations for vertical downward air-water flow at  $U_{SL}$  of 0.02m/s

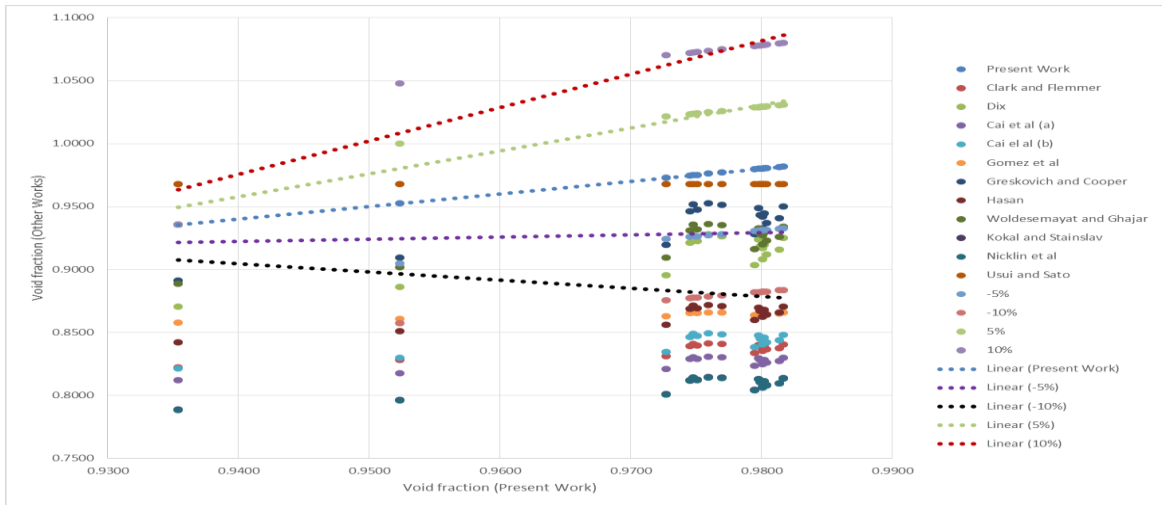


**Fig 4.7(c):** performance of 11 correlations for vertical upward air-water flow at  $U_{SL}$  of 0.04m/s

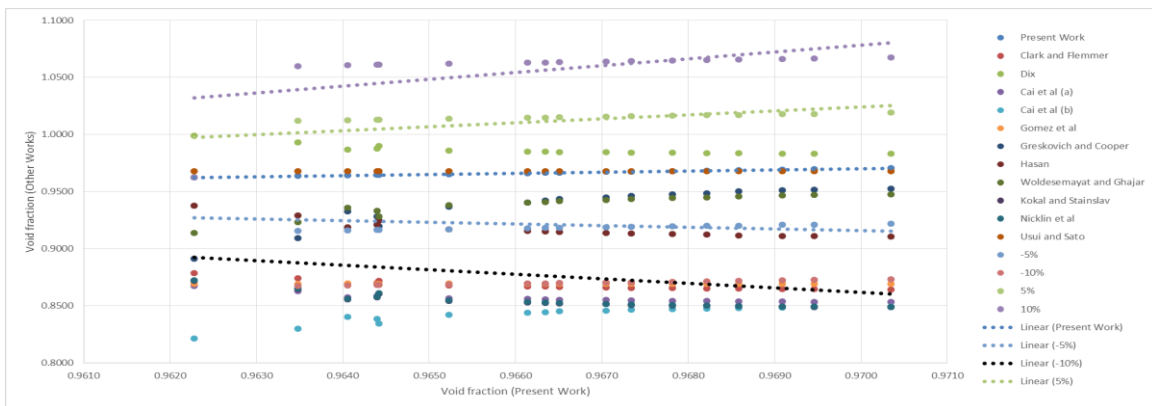


**Fig 4.7(d):** performance of 11 correlations for vertical downward air-water flow at  $U_{SL}$  of 0.04m/s

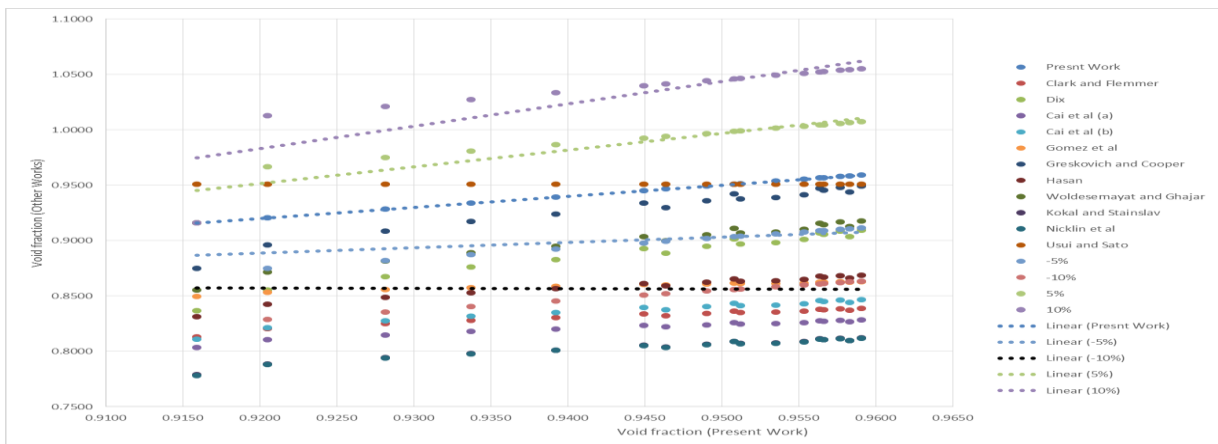


**Fig 4.7(e):** performance of 11 correlations for vertical upward air-water flow at  $U_{SL}$  of 0.08m/s

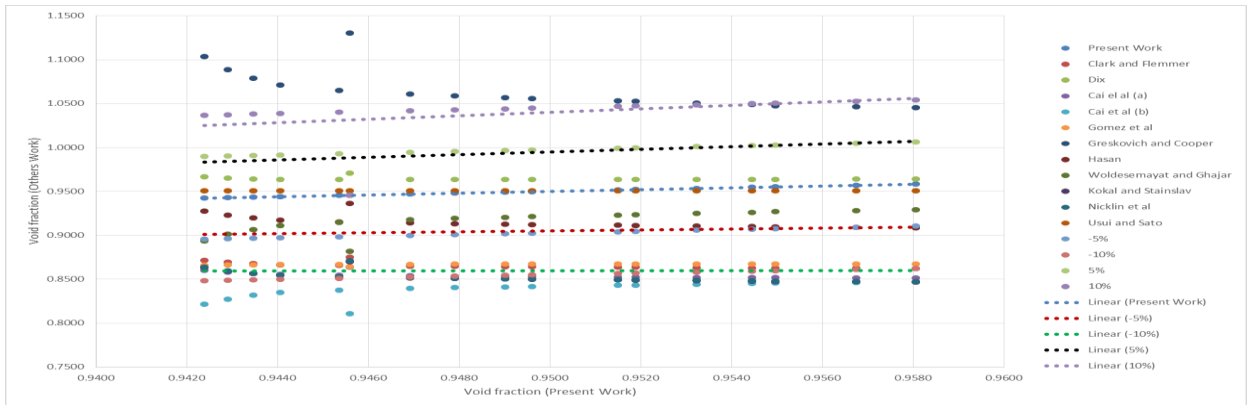


**Fig 4.7(f):** performance of 11 correlations for vertical downward air-water flow at  $U_{SL}$  of 0.08m/s

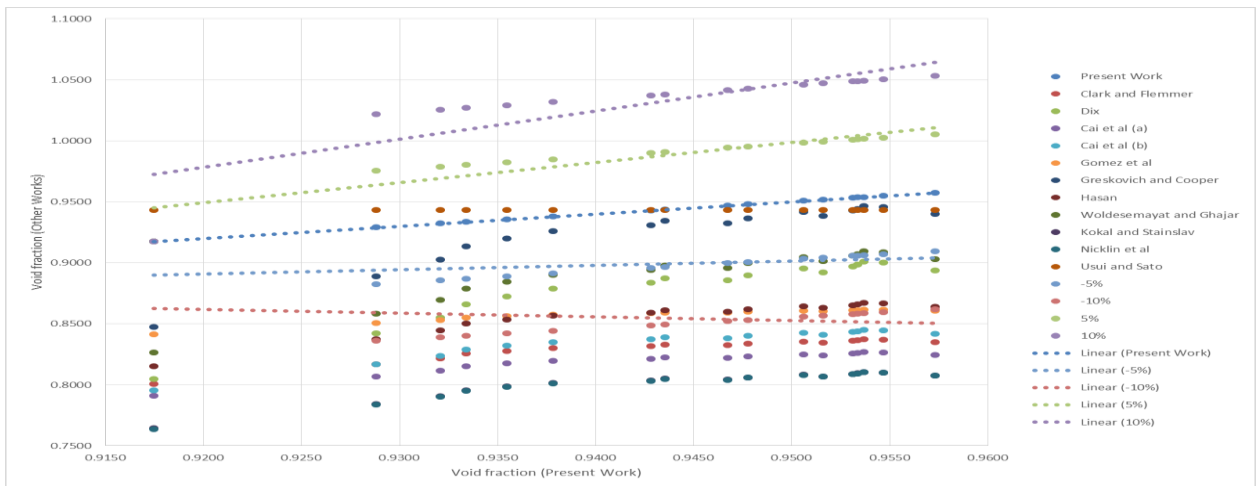


**Fig 4.7(g):** performance of 11 correlations for vertical upward air-water flow at  $U_{SL}$  of 0.1m/s

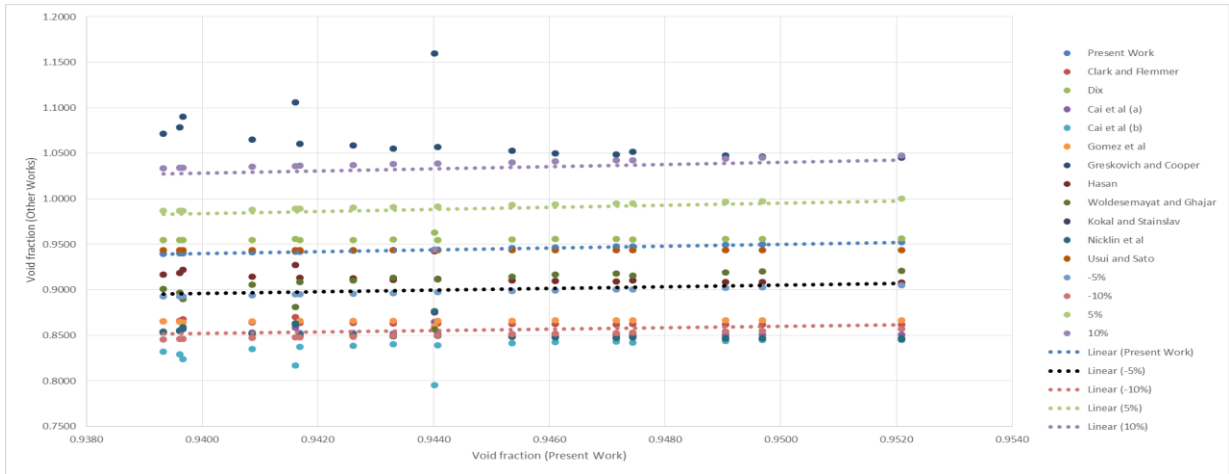


**Fig 4.7(h):** performance of 11 correlations for vertical downward air-water flow at  $U_{SL}$  of 0.1m/s

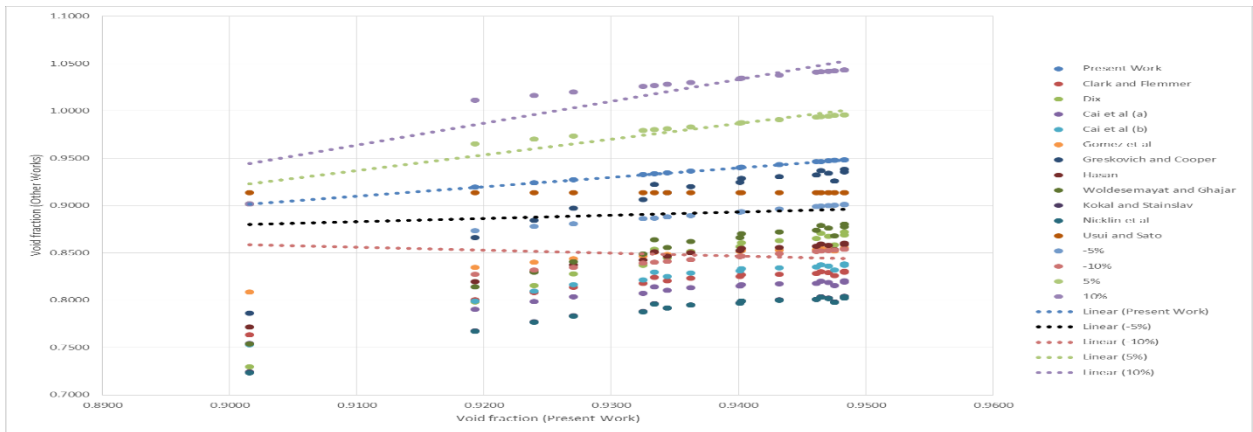


**Fig 4.7(i):** performance of 11 correlations for vertical upward air-water flow at  $U_{SL}$  of 0.2m/s

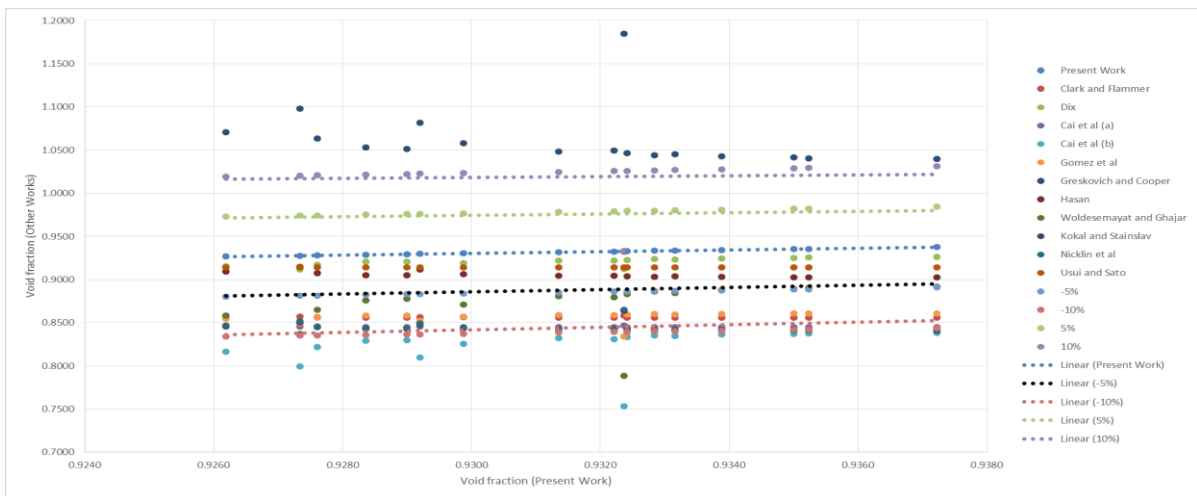


**Fig 4.7(j):** performance of 11 correlations for vertical downward air-water flow at  $U_{SL}$  of 0.2m/s

**4.8 Root Mean Error:**

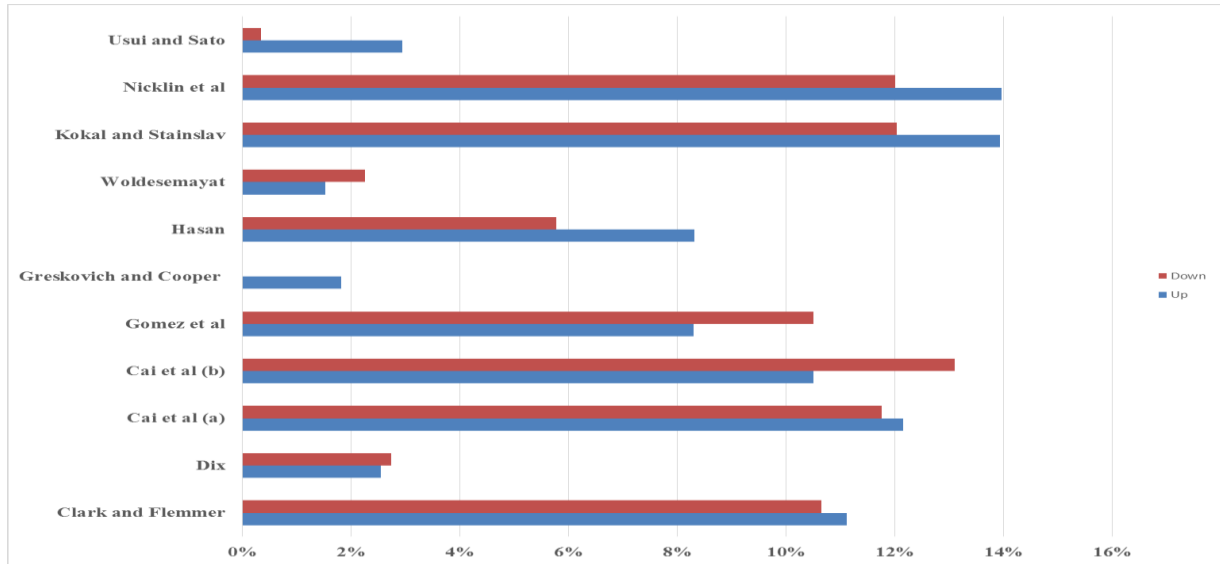


**Fig 4.8 (a):** RMSE value for 11 correlations for Up and down flow for  $U_{SL}=0.02m/s$

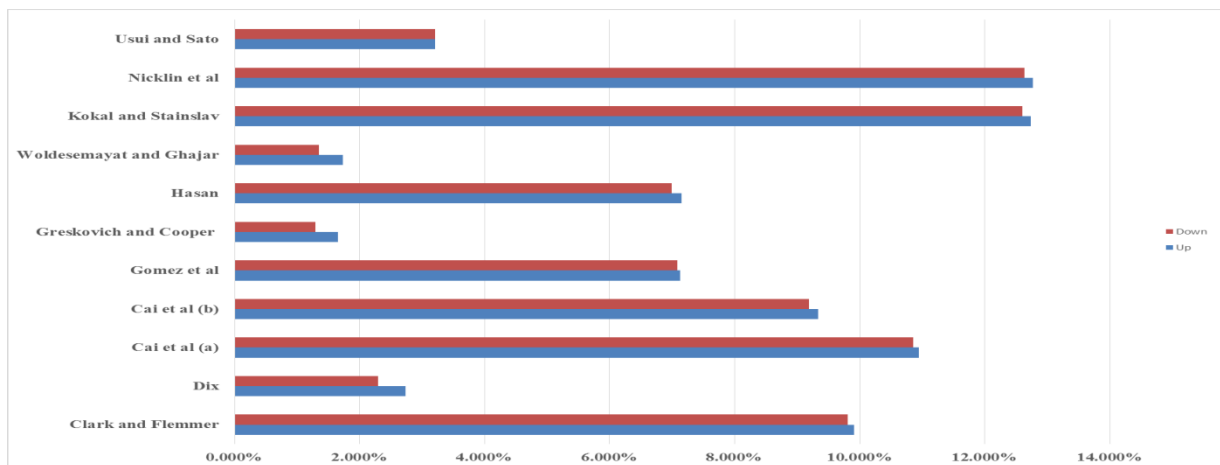


Fig 4.8(b): RMSE value for 11 correlations for Up and down flow for  $U_{SL}=0.04\text{m/s}$

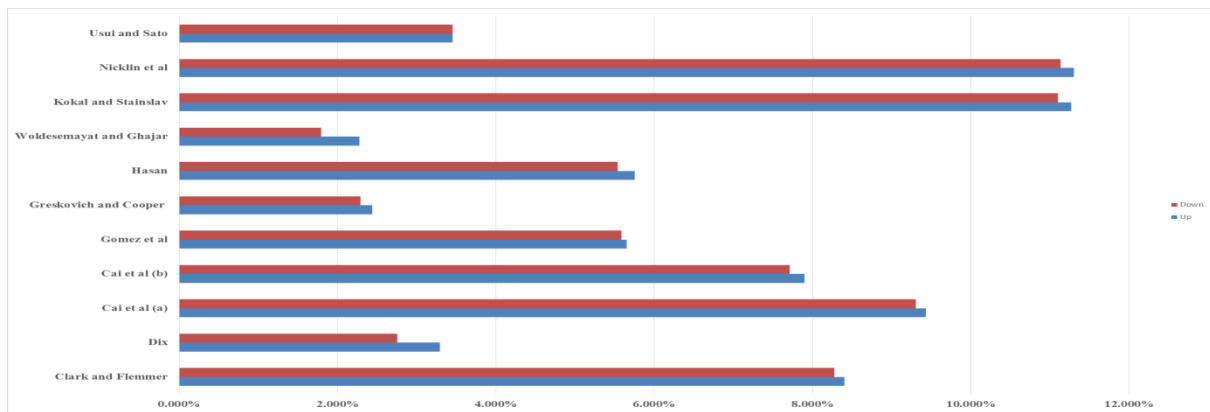


Fig 4.8(c): RMSE value for 11 correlations for Up and down flow for  $U_{SL}=0.08\text{m/s}$

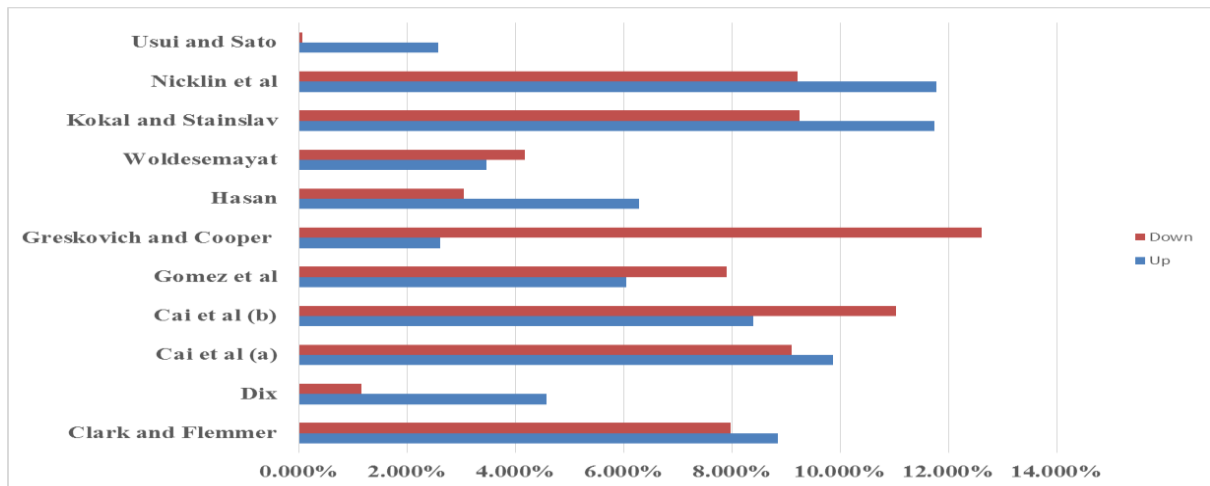


Fig 4.8(d): RMSE value for 11 correlations for Up and down flow for  $U_{SL}=0.1\text{m/s}$

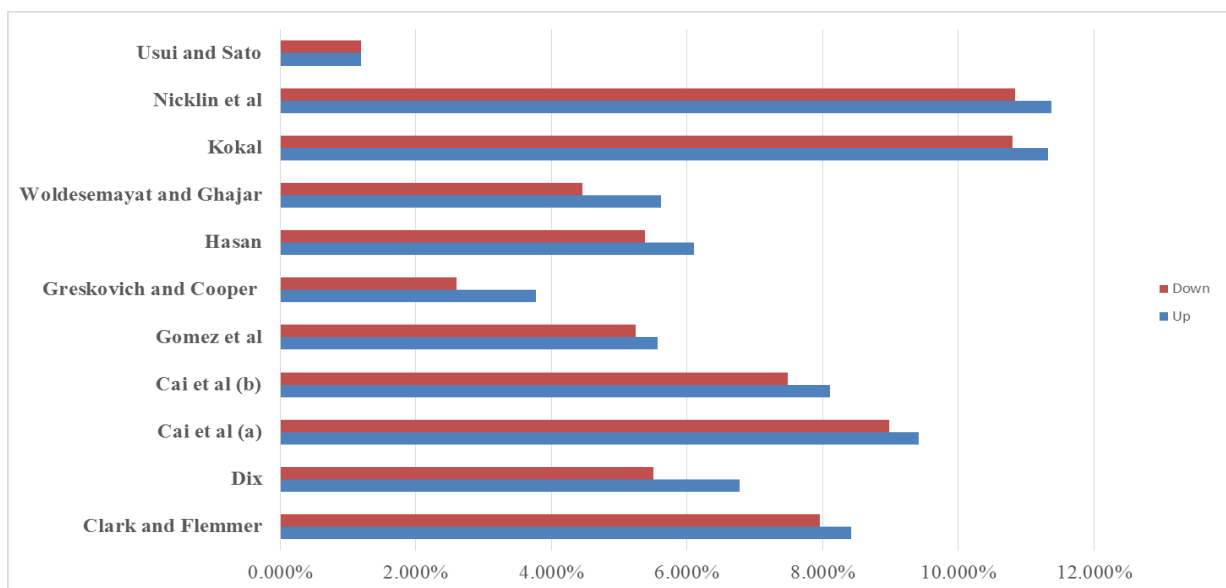


Fig 4.8(e): RMSE value for 11 correlations for Up and down flow for  $U_{SL}=0.2\text{m/s}$

**Table 4.3:** Comparison of prediction of void fraction correlations in vertical upward air-water flow

Correlations	Percentage of data points within										RMSE%				
	$\pm 5\%$					$\pm 10\%$					0.02	0.04	0.08	0.1	0.2
	0.02	0.04	0.08	0.1	0.2	0.02	0.04	0.08	0.1	0.2					
(Clark & Flemmer, 1985)	0	0	0	0	0	0	0	0	0	0	11	9.9	8.4	8.8	8.4
(Dix, 1971)	100	93	94.1	94.1	76.5	100	93	94.1	94.1	76.5	3	2.7	3.3	4.6	6.8
(Cai et al., 1997) bubbly flow	0	0	0	0	0	0	0	0	0	0	12	10.9	9.4	9.9	9.4
(Cai et al., 1997) slug flow	0	0	0	0	0	0	0	0	0	0	11	9.3	7.9	8.4	8.1
(Gomez et al., 2000)	0	0	76.5	70.5	64.5	0	0	76.5	70.5	64.5	8	7.1	5.7	6.0	5.6
(Greskovich & Cooper, 1975)	94.1	94.1	100	94.1	94.1	94.1	94.1	100	94.1	94.1	2	1.6	2.4	2.6	3.8
(Hasan, 1995)	0	0	76.5	70.5	76.5	0	0	76.5	70.5	76.5	8	7.1	5.8	6.3	6.1
(Woldesemayat & Ghajar, 2007)	94.1	94.1	100	94.1	76.5	94.1	94.1	100	94.1	76.5	2	1.7	2.3	3.5	5.6
(Kokal & Stanislav, 1989)	0	0	0	0	0	0	0	0	0	0	14	12.7	11.3	11.7	11.3
(Nicklin et al.,	0	0	0	0	0	0	0	0	0	0	14	12.8	11.3	11.8	11.4

1962)															
(Usui & Sato, 1989)	94.1	94.1	100	100	100	94.1	94.1	94.1	100	100	3	3.2	3.5	2.6	1.2

**Table 4.4:** Comparison of prediction of void fraction correlations in vertical downward air-water flow

Correlations	Percentage of data points within										RMSE%				
	$\pm 5\%$					$\pm 10\%$					0.02	0.04	0.08	0.1	0.2
	0.02	0.04	0.08	0.1	0.2	0.02	0.04	0.08	0.1	0.2					
(Clark & Flemmer, 1985)	0	0	100	100	100	0	0	100	100	100	11	9	8	7.8	8.0
(Dix, 1971)	100	100	100	100	100	100	100	100	100	100	3	2	2	1.2	1
(Cai et al., 1997) bubbly flow	0	0	0	0	0	0	0	0	0	0	12	11	9	9.1	9
(Cai et al., 1997) slug flow	0	0	0	0	0	0	0	0	0	0	13	12	11	11	11
(Gomez et al., 2000)	0	0	100	100	100	0	0	100	100	100	10	9	8	7.9	8
(Greskovich & Cooper, 1975)	-	0	29.4	0	0	-	0	29.4	0	0	-	3	12	12.6	13
(Hasan, 1995)	100	100	100	100	100	100	100	100	100	100	6	5	3	3.1	3
(Woldesemayat & Ghajar, 2007)	100	100	100	100	100	100	100	100	100	100	2	3	3	4.2	7
(Kokal & Stanislav,	0	0	0	0	0	0	0	0	0	0	12	11	9	9.3	7

1989)															
(Nicklin et al., 1962)	0	0	5.88	30	52.9	0	0	5.88	30	52.9	12	11	9	9.2	9
(Usui & Sato, 1989)	100	100	100	100	100	100	100	100	100	100	0.01	1	0.01	0.07	2

From the trend of the figures and tables presented above, the accuracy and the performance of the void fraction correlations is judged in terms of the absolute error and RMS error. Since literature does not give universal definition for satisfactory performance of the correlations the trend reported in table 4.3 and 4.4 will be used for upward and downward flow respectively. In vertical upward flow, it can be observed that none of the data points predicted by using (Clark & Flemmer, 1985), (Cai et al., 1997) bubbly flow and slug flow (Kokal & Stanislav, 1989), and (Nicklin et al., 1962) didn't fall within  $\pm 5\%$  and  $\pm 10\%$  and RMS is  $> 8\%$ . (Hasan, 1995) data points didn't fall within  $\pm 5\%$  and  $\pm 10\%$  at  $U_{SL}$  of 0.02-0.4m/s but at least 70% of the data fall with from 0.08-0.2m/s with  $RMS < 8\%$ . Also (Gomez et al., 2000) data point didn't fall within  $\pm 5\%$  and  $\pm 10\%$   $U_{SL}$  of 0.02-0.4m/s but at least 60% of the data fall with from 0.08-0.2m/s with  $RMS \geq 5.6\%$ . (Cai et al., 1997) could not give good prediction because it is developed for bubbly flow and slug flow respectively. The correlation of (Greskovich & Cooper, 1975), (Dix, 1971), (Woldesemayat & Ghajar, 2007) and (Usui & Sato, 1989) gives best performance as at least 90% of data points predicted fall within  $\pm 5\%$  and  $\pm 10\%$  and  $RMS < 4\%$ . In vertical downward flow, it can be observed that none of the data points predicted by using (Cai et al., 1997) bubbly flow and slug flow, (Greskovich & Cooper, 1975) and (Kokal & Stanislav, 1989) didn't fall within  $\pm 5\%$  and  $\pm 10\%$  and RMS is  $> 8\%$ . (Clark & Flemmer, 1985) data points didn't fall within  $\pm 5\%$  and  $\pm 10\%$  at  $U_{SL}$  of 0.02-0.4m/s but 100% of the data fall within from 0.08-0.2m/s with  $RMS < 8\%$ , (Gomez et al., 2000) data points didn't fall within  $\pm 5\%$  and  $\pm 10\%$  at  $U_{SL}$  of 0.02-0.4m/s but 100% of the data fall within from 0.08-0.2m/s with  $RMS < 8\%$ . (Nicklin et al., 1962) data points didn't fall within  $\pm 5\%$  and  $\pm 10\%$  at  $U_{SL}$  of 0.02-0.4m/s but at least 6% of the data fall within from 0.08-

0.2m/s with RMS>8%. (Cai et al., 1997) bubbly flow and slug flow could not give good prediction because it is developed for bubbly flow and slug flow respectively. The correlation of (Dix, 1971), (Woldesemayat & Ghajar, 2007), (Hasan, 1995) and (Usui & Sato, 1989) gives best performance as 100% of data points predicted fall within  $\pm 5\%$  and  $\pm 10\%$  and RMS  $\leq 7\%$ .

#### **4.9: Validation of the Constitutive Equations for $C_o$ and $U_{GM}$ :**

Out of 5 constitutive equations for distribution parameters cited in this available for large pipes cited in this work it can be observed that only (Kawanishi et al., 1990) and (Hirao et al., 1986) that gave a better approximation at  $U_{SL}$  of 0.02-0.08 with absolute error of 10% with Close to 1 as observed by (Bhagwat & Ghajar, 2012a) that as the flow is moving towards annular flow the  $C_o$  tends to one whereas at  $U_{SL}$  of 0.1-0.2% the absolute error is 12%. For downward flow, the absolute error given by (Hirao et al., 1986)) and (Kawanishi et al., 1990) in respect to the experimental value is 11% at  $U_{SL}$  of 0.02- whereas the absolute error at  $U_{SL}$  0.04-0.2 gave absolute error >11%.

Out of the eight constitutive equations cited in this work available for drift velocity in large diameter pipes it can be observed that in vertical upward flow the equation of (Hirao et al., 1986) , (Kawanishi et al., 1990), (Ishii, 1977) , combination of (Clark & Flemmer, 1985) and (Hirao et al., 1986) , (Haramathy, 1960) and (Goda et al., 2003) gives absolute error of 2%, 2%, 1%, 1% and 2% respectively at  $U_{SL}$  of 0.04m/s.(Hibiki & Ishii, 2003) and (Hirao et al., 1986) also gave absolute error of 3% at  $U_{SL}$  of 0.08m/s. while in downward flow it can be observed that (Hirao et al., 1986), (Kawanishi et al., 1990), (Ishii, 1977) and (Goda et al., 2003) gives absolute error of 10% at  $U_{SL}$  of 0.08m/s. The table showing the trend of these values is available in the appendix.

It is observed that the huge discrepancy in the constitutive equations available for upward and downward diameter flows in large diameter pipe and the experimental result maybe a

result of pipe diameter, gas and liquid flow rates, flow patterns and fluid combinations under which their experiments were conducted.

## CHAPTER 5

### Conclusion:

In this work, the result of the experiment carried out air-water flow in vertical upward and downward flow of 127mm diameter pipe was analysed in terms of the flow pattern and void fraction values and follow the same trend as that of literatures cited. Flow regime map for both pipe orientations has been plotted using Sholam's flow pattern map. The following conclusion can be made based on the measured data:

- The flow regime for the vertical upward and downward air-water flow in the 127mm diameter pipe over a range of gas and liquid superficial velocity of (3.45-10.1)m/s and (0.02-0.2)m/s respectively is annular flow which is characterised by high void fraction both from the time series and PDF.
- The differences between vertical downward and upward two-phase flow observed from the plot of average void fraction against superficial velocity were as result of the buoyancy, gravity and liquid inertia which is also observed in the work of (Bhagwat & Ghajar, 2012b).
- The dominant frequency depends on the gas superficial velocity at low liquid superficial velocities and shows a wide variation in the up and down air-water flow but dependency becomes weak as the liquid superficial velocity approaches 0.1m/s and 0.2m/s and no clear difference in terms of pipe orientations.
- The drift-flux model can be used to predict the cross-sectional and time averaged void fraction for annular flow in both upward and downward two-phase flow. This equation gives a distribution coefficient close to 1 and drift velocity approaching zero as it is always for high void fraction regime in either vertical upward and downward two-phase flow.
- The momentum equation developed by (Usui & Sato, 1989) for small diameter pipe aside the drift-flux model using two parameters the Froude number ( $F_{rf}$ ) which is a

function of the liquid superficial velocity and wall friction factor ( $C_w$ ) for annular/falling films for small pipes was able to give a good prediction for downward and upward annular flow using 127mm pipe size with data point of at least 90% fall within  $\pm 5\%$  and  $\pm 10\%$  with RMS of at most 7% compared to that of 203.2mm diameter pipe reported by (Wang, Li, Yousaf, et al., 2018).

- The best performing correlations for upward flow are correlation of (Greskovich & Cooper, 1975), (Dix, 1971), (Woldesemayat & Ghajar, 2007) and (Usui & Sato, 1989) of at least 90% of data points predicted fall within  $\pm 5\%$  and  $\pm 10\%$  and RMS  $< 4\%$ .
- The best performing correlations for downward flow are correlation of (Dix, 1971), (Woldesemayat & Ghajar, 2007), (Hasan, 1995) and (Usui & Sato, 1989) as 100% of data points predicted fall within  $\pm 5\%$  and  $\pm 10\%$  and RMS  $\leq 7\%$ .
- The huge discrepancy in the constitutive equations available for upward and downward diameter flows in large diameter pipe and the experimental result maybe a result of pipe diameter, gas and liquid flow rates, flow patterns and fluid combinations under which their experiments were conducted.

## REFERENCES

- Abdulkadir, M., Mbalisigwe, U. P., Zhao, D., Azzopardi, B. J., & Tahir, S. (2019). Characteristics of Churn and annular flows in a large diameter vertical riser. *International Journal of Multiphase*, 1–14.
- Alireza, B. (2014). *Natural Gas Processing*.
- Almabrok, A. (2013). *Gas-Liquid Two-Phase Flow in Up and Down Vertical Pipes*.
- Bhagwat, S. M., & Ghajar, A. J. (2012a). Correlation for a Gas-Liquid Two Phase Flow Based on the Concept of Drift. *Heat Transfer Conference*, 1–10.
- Bhagwat, S. M., & Ghajar, A. J. (2012b). Similarities and differences in the flow patterns and void fraction in vertical upward and downward two phase flow. *Experimental Thermal and Fluid Science*, 39, 213–227. <https://doi.org/10.1016/j.expthermflusci.2012.01.026>
- Bouyahiaoui, H., Azzi, A., Saidj, F., & Zeghloul, A. (2008). Flow patterns of a vertically downward two phase flow. *International Journal of Heat and Mass Transfer*, 51, 3442–3459.
- Cai, J., Chen, T. Q., & Ye. (1997). Void fraction in bubbly and slug flow in downward air-oil two-phase flow in vertical tubes. *International Symposium on Multiphase Flow*.
- Capovilla, M. S., Coutinho, R. P., de Sousa, P. C., & Waltrich, P. J. (2019). Experimental investigation of upward vertical two-phase high-velocity flows in large-diameter pipes. *Experimental Thermal and Fluid Science*, 493–505. <https://doi.org/10.1016/j.expthermflusci.2018.12.024>
- Clark, N. N., & Flemmer, R. L. (1985). *Predicting the Holdup in Two-Phase Bubble Up flow and Down flow Using the Zuber and Findlay Drift-Flux Mode*. 31(3), 500–503.
- COSTIGAN, G., & WHALLEY, P. B. (1997). SLUG FLOW REGIME IDENTIFICATION FROM DYNAMIC VOID FRACTION MEASUREMENTS IN VERTICAL AIR-WATER

- FLAWS. *International Journal of Multiphase Flow*, 23(2), 263–282.
- Dix, G. E. (1971). *Vapor Void Fractions for Forced Convection with Subcooled Boiling at Low Flow Rates*.
- Dong, F., Liu, X., Deng, X., Xu, D., & Xu, L. (2001). Identification of two-phase flow regimes in horizontal, inclined and vertical pipes. *Measurement Science and Technology*, 12, 1069–1075.
- Duns Jr, H., & Ros, N. C. J. (1963). Vertical flow of gas and liquid mixtures in wells. *In 6th World Petroleum Congress. World Petroleum Congress*.
- Goda, H., Hibiki, T., Kim, S., Ishii, M., & Uhle, J. (2003). Drift-flux model for downward two-phase flow. *International Journal of Heat and Mass Transfer*, 46(25), 4835–4844.  
[https://doi.org/10.1016/S0017-9310\(03\)00309-0](https://doi.org/10.1016/S0017-9310(03)00309-0)
- Godbole, P. V., Tang, C. C., & Ghajar, A. J. (2011). Comparison of void fraction correlations for different flow patterns in upward vertical two-phase flow. *Heat Transfer Engineering*, 32(10), 843–860. <https://doi.org/10.1080/01457632.2011.548285>
- Gomez, L. E., Shoham, O., Schmidt, Z., Chokshi, R. N., & Northug, T. (2000). Unified Mechanistic Model for SteadyState Two-Phase Flow. *Horizontal to Vertical Upward Flow, Society of Petroleum Engineers Journal*, 5(3), 339–350.
- Greskovich, E. J., & Cooper, W. T. (1975). Correlation and Prediction of Gas-Liquid Holdups in Inclined Upflows. *AIChE Journal*, 21(6), 1189–1192.
- Haramathy, T. Z. (1960). Velocity of large drops and bubbles in media of infinite or restricted extent. *AIChE*, 6, 281–288.
- Hasan, A. R. (1995). void fraction in bubbly and slug flow in downward vertical and inclined systems. *Society of Petroleum Engineers Production and Facilities*, 10(3), 172–176.
- Hernandez Perez, V. and Azzopardi, B. J. (2018). Effect of Inclination on Gas Liquid Flows.

10th Int. Conf. "Multiphase Flow in Industrial Plant, (September).

Hibiki, T., & Ishii, M. (2003). One-dimensional drift-flux model and constitutive equations for relative motion between phases in various two-phase flow regimes. *International Journal of Heat and Mass Transfer*, 46(25), 4935–4948. [https://doi.org/10.1016/S0017-9310\(03\)00322-3](https://doi.org/10.1016/S0017-9310(03)00322-3)

Hirao, Y., Kawanishi, K., Tsuge, A., & Kohriyama, T. (1986). Experimental study on drift flux correlation formulas for two-phase flow in large diameter tubes. *Proceedings of 2nd International Topical Meeting on Nuclear Power Plant Thermal Hydraulics and Operations*, 1-88-1–94.

Ishii, M. (1977). *One-Dimensional Drift-Flux Model and Constitutive Equations for Relative Motion Between Phases in Various Two-Phase Flow Regimes*.

Kanu, U. O. . (2013). *Characterisation of Churn Flow Coalesces (CFC) in Vertical Pipes*. University of Nottingham.

Kataoka, I., & Ishii, M. (1987). Drift Flux Model for Large Diameter Pipe and New Correlation for Pool Void Fraction. *International Journal of Heat and Mass Transfer*, 30(9), 1927–1939.

Kawanishi, K., Hirao, Y., & Tsuge, A. (1990). An experimental study on drift flux parameters for two-phase flow in vertical round tubes. *Nuclear Engineering and Design*, 120, 447–458.

Kokal, S. L., & Stanislav, J. F. (1989). An Experimental Study of Two-Phase Flow in Slightly Inclined Pipes—II. Liquid Holdup and Pressure Drop. *Chemical Engineering Science*, 44(3), 681–693.

Mokhatab, S., & Mak, J. Y. *Handbook of Natural Gas Transmission and Processing*. , (2015).

- Nicklin, D. J., Wilkes, J. O., & Davidson, J. F. (1962). Two-Phase Flow in Vertical Tubes. *Chemical Engineering Research and Design*, 40, 61–68.
- Omebere-Iyari, N. K., & Azzopardi, B. J. (2007). A study of flow patterns for gas/liquid flow in small diameter tubes. *Chemical Engineering Research and Design*, 85(2 A), 180–192. <https://doi.org/10.1205/cherd05059>
- Oshinowo, O. (1972). *Two-Phase Flow in a Vertical Tube*.
- Paras, G. (1982). *Characterization of downward two phase flow by neutron noise analysis*. University of Washington.
- Sharaf, S., van der Meulen, G. P., Agunlejika, E. O., & Azzopardi, B. J. (2016). Structures in gas-liquid churn flow in a large diameter vertical pipe. *International Journal of Multiphase Flow*, 78, 88–103. <https://doi.org/10.1016/j.ijmultiphaseflow.2015.09.005>
- Shen, X., Schlegel, J. P., Chen, S., Rassame, S., Griffiths, M. J., Hibiki, T., & Ishii, M. (2014). Flow Characteristics and Void Fraction Prediction in Large Diameter Pipes. *Frontiers & Progress in Multiphase Flow I*.
- Shoham, O. (2006). Mechanistic Modeling of Gas-Liquid Two-Phase Flow in Pipes. *Society of Petroleum Engineers*, 2006. Retrieved from <http://store.spe.org/Mechanistic-Modeling-of-Gas-Liquid-Two-Phase-Flow-in-Pipes-P36.aspx>
- Singer, M. (2017). *Trends in Oil and Gas Corrosion Research and Technologies*.
- Usui, K., & Sato, K. (1989). vertically downward two-phase flow (1) void distribution and average void fraction. *Journal of Nuclear Science and Technology*, 26(7), 670–680.
- Wang, G., Li, Z., Yang, X., & Ishii, M. (2018). Vertical Downward Two-phase Flow in a Large Diameter Pipe. *Transactions of the American Nuclear Society*, 117, 507–508.
- Wang, G., Li, Z., Yousaf, M., Yang, X., & Ishii, M. (2018). Experimental study on vertical downward air-water two-phase flow in a large diameter pipe. *International Journal of*

*Heat and Mass Transfer*, 118, 919–930.

<https://doi.org/10.1016/j.ijheatmasstransfer.2017.11.065>

Woldesemayat, M. A., & Ghajar, A. J. (2007). Comparison of Void Fraction Correlations for Different Flow Patterns in Horizontal and Upward Inclined Pipes. *International Journal of Multiphase Flow*, 33(4), 347–370.

Yamazaki, Y., & Yamaguchi, K. (1979). Characteristics of two-phase downflow in tubes: flow pattern, void fraction and pressure drop. *Journal of Nuclear Science and Technology*, 16(4), 245–255.

Yang, Z., Dang, Z., Yang, X., Ishii, M., & Shan, J. (2018). Downward two-phase flow experiment and general flow regime transition criteria for various pipe sizes. *International Journal of Heat and Mass Transfer* 125, 179–189.

Yijun, J., & Rezkallah, K. (1993). A study on void fraction in vertical co-current upward and downward two-phase flow gas-liquid flow-I: experimental results. *Chemical Engineering Communication*, 221–243.

Zuber, N., & Findlay, J. (1965). Average volumetric concentration in two-phase flow systems. *Journal of Heat Transfer*, 87(4), 453–468.